The Primacy of Magnitude in Low-Rank Adaptation

Zicheng Zhang[1]* **Haoran Li**[2] **Yifeng Zhang**[1] **Guoqiang Gong**[1] **Jiaxing Wang**[1]
Junxing Hu[1] **Pengzhang Liu**[1] **Qixia Jiang**[1]

[1]JD.com
[2]University of Chinese Academy of Sciences

Abstract

Low-Rank Adaptation (LoRA) offers a parameter-efficient paradigm for tuning large models. While recent spectral initialization methods improve convergence and performance over the naive "Noise & Zeros" scheme, their extra computational and storage overhead undermines efficiency. In this paper, we establish update magnitude as the fundamental driver of LoRA performance and propose LoRAM, a magnitude-driven "Basis & Basis" initialization scheme that matches spectral methods without their inefficiencies[1]. Our key contributions are threefold: *(i) Magnitude of weight updates determines convergence.* We prove low-rank structures intrinsically bound update magnitudes, unifying hyperparameter tuning in learning rate, scaling factor, and initialization as mechanisms to optimize magnitude regulation. *(ii) Spectral initialization succeeds via magnitude amplification.* We demystify that the presumed knowledge-driven benefit of the spectral component essentially arises from the boost in the weight update magnitude. *(iii) A novel and compact initialization strategy, LoRAM, scales deterministic orthogonal bases using pretrained weight magnitudes to simulate spectral gains*. Extensive experiments show that LoRAM serves as a strong baseline, retaining the full efficiency of LoRA while matching or outperforming spectral initialization across benchmarks.

1 Introduction

The rise of large pretrained models [1, 2, 3, 4, 5] has driven urgent needs for parameter-efficient fine-tuning (PEFT) methods [6, 7, 8, 9, 10, 11]. Among these, Low-Rank Adaptation (LoRA) [7] stands out for its *efficiency, flexibility, and stability*. By freezing pretrained weights and injecting trainable low-rank matrices, LoRA enables the update of less than 1% of the parameters, significantly reducing memory and compute costs. Its plug-and-play nature achieves easy integration into diverse models, facilitating model sharing and federated learning [12, 13]. Additionally, LoRA helps prevent catastrophic forgetting [14], making it well-suited for continual learning. These advantages have led to its wide adoption in multilingual NLP [15, 16, 17, 18] and multimodal applications [19, 20, 21, 22].

Despite achieved efficiency, the low-rank reparameterization constrains practical performance and convergence [14]. Besides the well-known "representation bottleneck" [23, 10, 24, 25, 26, 27, 28, 29], LoRA is highly sensitive to hyperparameters due to the non-convex and non-smooth loss landscape [30]. Effective training relies on careful tuning of rank [31, 32, 33], scaling factor [34], learning rate [35], initialization strategies [36, 37, 30], and preconditioning [30, 38, 39]. Recent works increasingly leverage information from pretrained weights [40, 41, 42] or task-specific data [43, 44, 39] to improve the "Noise & Zeros" baseline. Among these, PiSSA [40] pioneers the use of Singular Value Decomposition (SVD) for LoRA initialization, employing spectral components of pretrained

*Corresponding author: zhangzicheng6@jd.com
[1]Code is available here

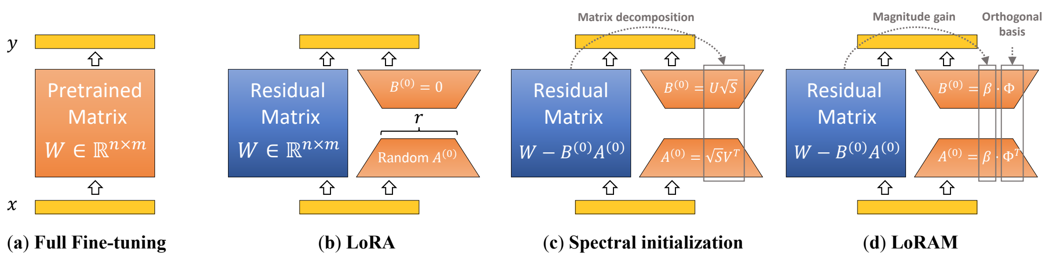
y
x
Pretrained Matrix $W \in \mathbb{R}^{n \times m}$
Residual Matrix $W \in \mathbb{R}^{n \times m}$
$B^{(0)} = 0$
r
Random $A^{(0)}$
Matrix decomposition
Residual Matrix $W - B^{(0)}A^{(0)}$
$B^{(0)} = U\sqrt{S}$
$A^{(0)} = \sqrt{S}V^T$
Magnitude gain
Orthogonal basis
Residual Matrix $W - B^{(0)}A^{(0)}$
$B^{(0)} = \beta \cdot \Phi$
$A^{(0)} = \beta \cdot \Phi^T$
(a) Full Fine-tuning
(b) LoRA
(c) Spectral initialization
(d) LoRAM

Figure 1: We propose LoRAM, a magnitude-driven initialization method that enhances both the convergence and performance of LoRA while maintaining its efficiency. *Unlike spectral initialization, which precomputes and stores singular components* (U, V, S) [40], *LoRAM uses deterministic orthogonal bases and derives scaling from pretrained weight statistics.* This elegant simplification is grounded in our analysis of LoRA through a novel lens of magnitude dynamics, where we show that the benefits of spectral values in scaling weight update magnitude can be effectively approximated.

weights to significantly enhance convergence and performance. Subsequent works [41, 44, 42, 39, 43] extend to diverse matrix decompositions, fostering a wave of knowledge-driven initialization schemes.

While spectral initialization [40, 41, 44, 39, 43] showcases considerable promise in convergence and performance, two fundamental challenges persist. First, they introduce **complexity by requiring additional matrix decomposition and storage overhead**, undermining usage efficiency in resource-constrained settings [45, 25, 46] and hindering seamless integration with deep learning libraries [6, 47]. Second, **their success remains poorly understood**. The common justification [40, 41, 43, 48] that spectral components preserve features better than random alternatives lacks theoretical grounding. Although recent works [44, 39] suggest that some specific initialization may approximate full-parameter gradients, the non-convex nature of LoRA renders training dynamics unpredictable.

In this paper, we demystify the knowledge-driven intuition behind spectral initialization and reveal that its effectiveness primarily stems from the magnitude scaling of weight updates. We design a minimal "Basis & Basis" initialization strategy, which demonstrates comparable performance without the overhead of SVD operations. Specifically, our key contributions can be summarized as:

- We identify **weight update magnitude as a fundamental principle** for analyzing and improving LoRA's training dynamics. This principle unifies previously independent factors, such as learning rate, scaling, and initialization, revealing their shared ability to control weight update strength and achieve comparable amplification effects when properly configured.
- We demonstrate that **initialization scheme critically shapes LoRA's weight magnitude dynamics**. Theoretically, we prove that LoRA naturally produces smaller updates than full fine-tuning, which limits its convergence and expressiveness. Moreover, we show that spectral initialization amplifies updates, providing a principled explanation for its effectiveness beyond knowledge-driven intuition.
- Guided by the magnitude principle, we propose **Magnitude-driven Initialization (LoRAM)** to make LoRA initialization efficient again. LoRAM employs a logarithmic magnitude factor to retain the benefits of spectral scaling, while directly scaling deterministic orthogonal bases to eliminate the need for decomposition and storage. Extensive experiments on language and vision-language tasks establish LoRAM as a strong and practical baseline, surpassing prior initialization schemes.

2 Magnitude Principle for Characterizing LoRA Dynamics

2.1 Preliminaries and Notations

Given a pretrained weight matrix $W \in \mathbb{R}^{n \times m}$, LoRA [7] reparameterizes the forward pass as

$$y = Wx + W_{\text{LoRA}}x = Wx + \alpha(BA - B^{(0)}A^{(0)})x, \tag{1}$$

where $B \in \mathbb{R}^{n \times r}$, $A \in \mathbb{R}^{r \times m}$ are trainable low-rank matrices with $r \ll \min(n, m)$, and α scales the update magnitude. The initialization term $B^{(0)}A^{(0)}$ can be absorbed into W for the convenience, as illustrated in Figure 1(b). Given a loss function L, LoRA updates are computed as:

$$\nabla_A L = \alpha B^\top \frac{\partial L}{\partial y} x^\top = \alpha B^\top (\nabla_W L), \quad \nabla_B L = \alpha \frac{\partial L}{\partial y} x^\top A^\top = \alpha (\nabla_W L) A^\top. \tag{2}$$

Magnitude metric. To elucidate how LoRA affects the training process, we analyze the dynamics of the parameters A, B, and the resulting weight update W_{LoRA}. Specifically, we define the weight magnitude as $\nu[W_{\text{LoRA}}] = \frac{1}{mn}\|W_{\text{LoRA}}\|_F^2$, which serves as a central metric in our study. Assuming independent and zero-mean entries [49], the expected weight magnitude is given by $\mathbb{E}[\nu[BA]] = r\,\mathbb{E}[\nu[B]]\,\mathbb{E}[\nu[A]]$. In the asymptotic regime where m and n are large, $\nu[W_{\text{LoRA}}]$ is approximated with the variance of W_{LoRA}, and $\nu[BA] \approx r\,\nu[B]\,\nu[A]$. Our analysis is motivated by the fact that LoRA introduces no change to the pretrained weights initially, *i.e.*, $\nu[W_{\text{LoRA}}^{(0)}] = 0$, while its effect emerges gradually through training. Therefore, we use the term "magnitude" instead of "variance" to highlight the cumulative growth of W_{LoRA}. In Appendix B, we also present a theoretical insight showing that parameter magnitude is a key determinant of LoRA's expressiveness.

2.2 Effect of Hyperparameters on Update Magnitude

Let $\Delta W_{\text{LoRA}}^{(t)}$ denote the weight update at step t for LoRA framework, and $W_{\text{LoRA}}^{(t)} = \sum_{i=0}^{t-1} \Delta W_{\text{LoRA}}^{(i)}$ represent cumulative adaptation. Given a learning rate η, we expand $\Delta W_{\text{LoRA}}^{(t)}$ using gradient update rules, leading to the following formulations for the update magnitude[2]:

$$\Delta W_{\text{LoRA}}^{(t)} = \alpha\eta \left(B^{(t)}\nabla_A L^{(t)} + \nabla_B L^{(t)} A^{(t)} + \eta \nabla_B L^{(t)} \nabla_A L^{(t)} \right), \tag{3}$$

$$\text{and} \quad \nu[\Delta W_{\text{LoRA}}^{(t)}] \approx r\alpha^2\eta^2 \left(\nu[B^{(t)}]\nu[\nabla_A L^{(t)}] + \nu[\nabla_B L^{(t)}]\nu[A^{(t)}] \right). \tag{4}$$

These equations indicate the complex interplay of multiple hyperparameters, distinct from the full-parameter updates given by $\Delta W^{(t)} = -\eta \nabla_W L^{(t)}$. We investigate the interplay among the learning rate η, scaling factor α, and initialization magnitude, revealing a quantifiable equivalence relationship.

Proposition 1 (Parameter Scaling Equivalence)**.** *For LoRA layers defined in Eq.* (1)*, consider decomposing the scaling factor $\alpha = \alpha' \alpha_A \alpha_B$, where $\alpha', \alpha_A, \alpha_B \in \mathbb{R}^+$. Under the commonly used optimization frameworks with negligible numerical errors, the following parametrization schemes exhibit dynamical equivalence throughout training: For all iterations $t \geq 0$, $\Delta W_{\text{LoRA}}^{(t)} = \Delta \tilde{W}_{\text{LoRA}}^{(t)}$ and $W_{\text{LoRA}}^{(t)} = \tilde{W}_{\text{LoRA}}^{(t)}$, where $\tilde{A}^{(t)}$, $\tilde{B}^{(t)}$ and $\tilde{W}^{(t)}$ represent the re-parameterized versions.*

	Original	***SGD***	***Adam***
Representation	αBAx	$\alpha' \tilde{B}\tilde{A}x$	$\alpha' \tilde{B}\tilde{A}x$
Initialization	$A^{(0)} = A_{\textit{init}}, B^{(0)} = B_{\textit{init}}$	$\tilde{A}^{(0)} = \alpha_A A_{\textit{init}}, \tilde{B}^{(0)} = \alpha_B B_{\textit{init}}$	$\tilde{A}^{(0)} = \alpha_A A_{\textit{init}}, \tilde{B}^{(0)} = \alpha_B B_{\textit{init}}$
Learning Rates	$\eta_A > 0, \eta_B > 0$	$\eta_{\tilde{A}} = \alpha_A^2 \eta_A, \eta_{\tilde{B}} = \alpha_B^2 \eta_B$	$\eta_{\tilde{A}} = \alpha_A \eta_A, \eta_{\tilde{B}} = \alpha_B \eta_B$

Remarks. This equivalence underscores how hyperparameters collectively regulate update magnitude, effectively reducing the search space for optimal configurations. A striking implication is that, increasing η_B in LoRA+ [35] is identical to scaling α in RsLoRA [34] under the "Noise & Zeros" initialization, highlighting the critical role of initialization magnitude in shaping LoRA's training dynamics, which is rarely discussed in prior works. For the non-zero initialization, it is advisable to first adjust the initialization magnitudes and learning rates for moderate improvements, as modifying α inherently combines the effects of both and may result in drastic and unpredictable changes.

To demonstrate the joint effect of hyperparameters on LoRA dynamics, we conduct a controlled experiment using a 5-layer MLP with "Noise & Zeros" initialized LoRA layers, setting the intermediate dimension to 400 and the LoRA rank to 25. The network is trained on synthetic data under various hyperparameter settings, consequently using SGD and Adam optimizers with $\eta = 5 \times 10^{-5}$. As shown in Figure 2(a), all settings with $\alpha = 16$ result in identical loss trajectories and parameter evolution, confirming the theoretical predictions. In contrast, weight updates deviate significantly when using $\alpha = 1$ with η scaled by 4, indicating that equivalence holds only under specific rules.

2.3 Magnitude Limitation Rooted in Low-Rank Structure

Guided by the established equivalence framework, we fix $\alpha = 1$ to eliminate the interference of scaling factors, which is the most commonly-used configuration in practical implementation. In the following, we prove initialization magnitudes and other factors critically influence the weight update.

Proposition 2 (Parameter Magnitude Dynamics)**.** *Consider LoRA parameters updated with the same learning rate η. Assume: $A^{(0)} \sim \mathcal{N}(\mathbf{0}, \sigma_A^2 I)$, $B^{(0)} \sim \mathcal{N}(\mathbf{0}, \sigma_B^2 I)$, $\nabla_W L^{(t)} \sim \mathcal{N}(\mathbf{0}, \sigma_L^2 I)$, and*

[2]See Appendix for derivation and proof

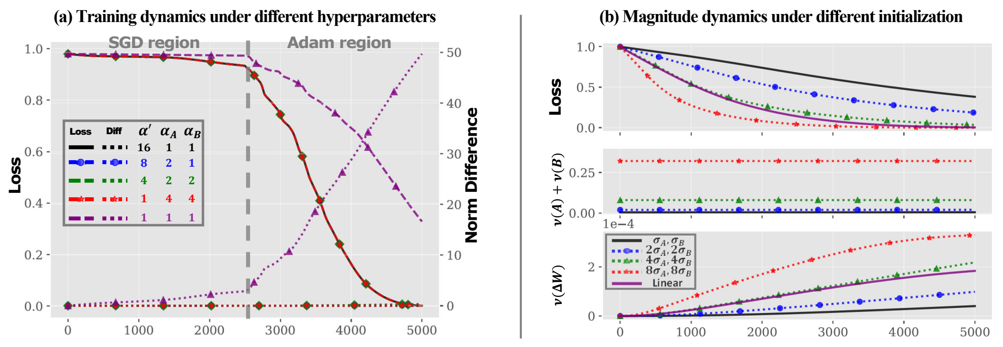

Figure 2: (a) Validation of Proposition 1. Each curve represents a model with unique hyperparameters. The norm difference (right axis) aggregates Frobenius norm discrepancies between the baseline model (black) and others across layers. Purple and other curves share identical learning rates but diverge due to differing initialization magnitudes. Equivalent optimization trajectories emerge from diverse hyperparameter combinations under both SGD and Adam optimizers. (b) Validation of Proposition 2. The black curve represents random orthogonal initialization. Parameter magnitudes are predominantly governed by initialization scaling, resulting in smaller weight changes compared to conventional linear layers. This necessitates the magnitude scaling in enhancing LoRA performance.

$\mathbb{E}[\langle A^{(t)}, \nabla_A L^{(t)}\rangle] = \mathbb{E}[\langle B^{(t)}, \nabla_B L^{(t)}\rangle] = 0$. *Under these conditions, the parameter magnitudes* $\boldsymbol{\nu}_t = \left[\mathbb{E}[\nu[A^{(t)}]], \mathbb{E}[\nu[B^{(t)}]]\right]^T$ *evolve as a linear dynamical system. Its exponential solution admits the linearized approximation under small-η regime:*

$$\boldsymbol{\nu}_t = \left(I + \begin{bmatrix} 0 & \gamma_B \\ \gamma_A & 0 \end{bmatrix}\right) \boldsymbol{\nu}_{t-1} \approx \begin{bmatrix} \sigma_A^2 + t\gamma_B\sigma_B^2 \\ \sigma_B^2 + t\gamma_A\sigma_A^2 \end{bmatrix}, \tag{5}$$

where $\gamma_A = m\eta^2\sigma_L^2$, $\gamma_B = n\eta^2\sigma_L^2$. *This further yields the evolution of weight update magnitude:*

$$\nu[W_{LoRA}^{(t)}] \approx k_1\gamma t + \mathcal{O}(\gamma^2 t^2), \text{ where } \gamma = \eta^2\sigma_L^2,\ k_1 = r(m\sigma_A^4 + n\sigma_B^4). \tag{6}$$

Remarks. This analysis uncovers essential properties of LoRA initialization and optimization trajectory. First, since γ_A and γ_B are very small values ($\ll 1$), the magnitudes of parameters $A^{(t)}$ and $B^{(t)}$ remains nearly unchanged throughout training, potentially constraining the representation capacity of the learned model. Moreover, unlike full-parameter tuning, which evolves at a linear rate of γ, *the low-rank structure introduces a proportional factor k_1, significantly slowing updates*. For instance, the naive "Noise & Zeros" initialization yields $k_1 = \frac{r}{m}$, while the dimension m in large models like LLaMA [3] is in the thousands or more. Despite the quadratic term accelerates growth, small gradients may temper this effect in the later training stages.

Figure 2(b) visualizes LoRA magnitude dynamics during training. We use the same network as in Figure 2(a) but apply a nonzero initialization with $\sigma_A = \sigma_B = \frac{1}{20}$. We explore a regular MLP with the same magnitude denoted as "Linear", and a group of networks with larger initialization magnitudes. Notably, while the loss decreases significantly, the magnitudes of A and B remain nearly unchanged throughout training. The magnitude evolution of W reveals that the basic LoRA with theoretically $k_1 = \frac{1}{16}$, grows substantially slower than the regular MLP. Increasing the initialization magnitude effectively accelerates the growth of W, aligning with our theoretical analysis.

Integrating analyses in this section, we derive a **magnitude principle** for LoRA development:

A valid improvement to LoRA convergence will enhance weight update magnitude $\nu[W_{LoRA}]$.

As shown in Proposition 2, magnitude principle could unify and explain improvement factors in existing works, including the learning rate, scaling factor, gradients, rank and initialization schemes.

3 Demystifying Spectral Gains with Magnitude Principle

The sheer scale of modern neural networks complicates the determination of optimal LoRA initialization across layers. Drawing inspiration from recent spectral initialization methods [40, 41, 43, 44, 39], which have demonstrated improved convergence and task performance, we reinterpret their effectiveness through the lens of the magnitude principle and introduce a magnitude-driven initialization

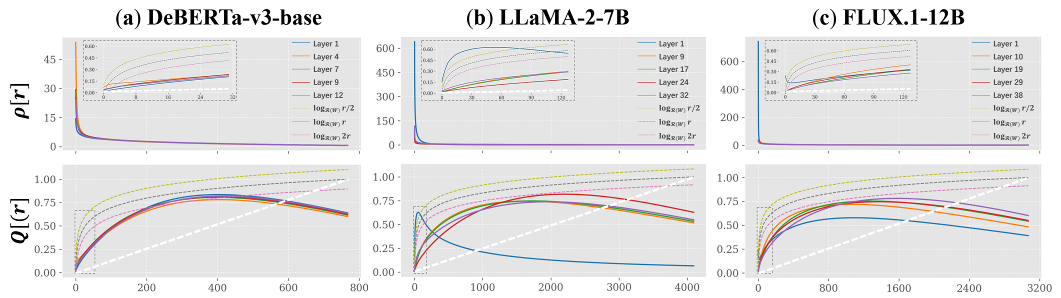

Figure 3: Illustration of spectral gain factor $Q[r]$ defined in Eq. (10) and spectral concentration factor $\rho[r]$ defined in Eq. (8) across DeBERTa-v3-base [50], LLaMA-2-7B [3] and FLUX.1-12B [51]. Values are computed from uniformly sampled layers. The white dotted line represents the linear growth rate of naive LoRA weight magnitudes, while spectral initialization exhibits faster growth. Due to its concave nature, we approximate the spectral gain factor using a logarithmic function.

method called LoRAM. Notably, these methods requires extra SVD computations and storage, leading to increased resource overhead and implementation complexity. In contrast, LoRAM mitigates these drawbacks and achieves even better performance. In the following, we take the seminal work PiSSA [40] as a representative baseline and ablate other methods in experiments (see Section 4.3).

3.1 Magnitude Gain in Spectral Initialization

The PiSSA method [40] initializes LoRA using the spectral decomposition of pretrained weight matrix $W = USV^\top$, which has a rank of $\mathcal{R}[W]$. The spectral initialization is defined as:

$$A^{(0)} = A_{\text{SVD}} = \sqrt{S_r} V_{:,:r}^\top, \quad B^{(0)} = B_{\text{SVD}} = U_{:,:r}\sqrt{S_r}, \tag{7}$$

where $S_r \in \mathbb{R}^{r\times r}$ contains the top-r singular values, and $U \in \mathbb{R}^{n\times n}$, $V \in \mathbb{R}^{m\times m}$ are the left and right singular vector matrices. While prior works [40, 41, 43, 48] attribute PiSSA's success to its ability to preserve principal components, we show that its key advantage lies in singular value weighting. By redistributing dominant variance into the initialization, PiSSA facilitates adaptive magnitude updates across layers, accelerating convergence.

Consider the statistics of the top-r singular values, we define the spectral concentration factor as:

$$\rho[r] \triangleq \frac{\mathbb{E}_r[s]^2}{\mathbb{E}_{\mathcal{R}[W]}[s^2]} = \frac{\left(\frac{1}{r}\sum_{i=1}^r s_i\right)^2}{\frac{1}{\mathcal{R}[W]}\sum_{i=1}^{\mathcal{R}[W]} s_i^2}. \tag{8}$$

This factor captures the concentration of energy in the top-r singular values. We then reformulate

$$\nu(A_{\text{SVD}}) = \mathbb{E}_r[s]\nu[V_{:,:r}] = \sqrt{\frac{n\rho[r]\nu[W]}{m\mathcal{R}[W]}},\ \nu(B_{\text{SVD}}) = \mathbb{E}_r[s]\nu[U_{:,:r}] = \sqrt{\frac{m\rho[r]\nu[W]}{n\mathcal{R}[W]}}. \tag{9}$$

Essentially, $\rho[r]$ acts as a scaling factor that redistributes variance from the pretrained weight matrix, influencing the magnitude of updates during training. Since $\rho[r]$ monotonically decreases with r, its impact is more pronounced for smaller r, making it particularly relevant for LoRA applications.

Spectral Gain Factor. Taking the above magnitudes into the dynamics in Eq. (6) further derives:

$$k_1 = Q[r](m+n)\nu[W], \quad 0 \le Q[r] \triangleq \frac{\rho[r]r}{\mathcal{R}[W]} \le 1. \tag{10}$$

Given that $\nu[W] \sim \mathcal{O}(\min(\frac{1}{m}, \frac{1}{n}))$, this results in a gain factor of at least $Q[r]$, which we term as the "spectral gain factor". As shown in Figure 3, the spectral gain factor $Q[r]$ exhibits bounded variation in $[0, 1]$ with characteristic concavity, which can be formally derived via Jensen's inequality. Although SVD components are not completely independent preventing the theoretical monotonic increase in $Q[r]$, this concavity also suggests that the gain effect is more pronounced when r is small, reinforcing the effectiveness of spectral initialization for LoRA in the parameter-efficient manner.

3.2 Efficient Magnitude-driven Initialization with LoRAM

We propose LoRAM to achieve similar magnitude update rate in Eq. (10) like PiSSA while eliminating spectral computation. As depicted in Algorithm 1, LoRAM initializes the parameter matrices as:

$$A^{(0)} = A_{\text{LoRAM}} = \beta\cdot\Phi_m^\top, \quad B^{(0)} = B_{\text{LoRAM}} = \beta\cdot\Phi_n, \quad \beta = \left(\frac{Q[r]\cdot\nu[W]}{\nu[\Phi_n\Phi_m^\top]}\right)^{\frac{1}{4}}. \tag{11}$$

Algorithm 1 LoRAM Initialization Procedure

```
Input: Pretrained weight $W \in \mathbb{R}^{n \times m}$, target rank $r$
Output: Initialized parameters $A^{(0)}, B^{(0)}, W$
$\Phi_n$, $\Phi_m \leftarrow$ get_basis(n, r), get_basis(m, r)        ▷ Generate basis matrices, e.g., Eq (12)
$\beta \leftarrow \left(\frac{\log_{\min(n,m)}(r) \cdot \nu[W]}{\nu[\Phi_n \Phi_m^\top]}\right)^{1/4}$        ▷ Compute magnitude gain factor
$B^{(0)}, A^{(0)}, W \leftarrow \beta \cdot \Phi_n, \beta \cdot \Phi_m^\top, W - \beta^2 \cdot \Phi_n \Phi_m^\top$        ▷ Initialize parameters
```

Here Φ_n and Φ_m denote the first r columns of an n- and m-dimensional orthogonal basis matrices, respectively. Given that $\nu[\Phi_n] = \frac{1}{n}$ and $\nu[\Phi_m] = \frac{1}{m}$, LoRAM achieves the similar magnitude as PiSSA with $k_1 = Q[r](m+n)\nu[W]$. We can also derive $\nu[B^{(0)}A^{(0)}] = Q[r]\nu[W]$, implying LoRAM inherently ensures numerical stability and moderate corrections to the pretrained weight.

Logarithmic Gain Factor. Due to the concave nature of $Q[r]$, we approximate its analytical form using an asymptotic expansion: $Q[r] \approx \log_{\min(n,m)}(r)$. As illustrated in Figure 3, this logarithmic function effectively captures the monotonic increase nature, providing a predictable improvement than LoRA and PiSSA particularly when using a small rank r.

Deterministic Basis Matrix. To eliminate the need for storing initialization buffers, we adopt an analytic approach instead of random initialization. Specifically, we employ the Discrete Sine Transform (DST) basis due to its simplistic mathematical definition:

$$\Phi_m[i,j] = \sqrt{\frac{2}{m+1}} \sin\left(\frac{(i+1)(j+1)\pi}{m+1}\right), \quad 0 \le i, j < m. \tag{12}$$

This formulation constructs orthogonal matrices of arbitrary dimensions, ensuring reproducibility across different devices while providing provable statistical properties: $\mathbb{E}[\Phi_m] = 0$ and $\nu[\Phi_m] = \frac{1}{m}$. One may wonder if randomness is required for initialization, we find it unnecessary in LoRA. In fact, DST even slightly outperforms random strategies in our ablation experiments (see Section 4.3).

Efficiency and Compatibility. Since β and Φ avoid complex matrix operations, LoRAM retains the efficiency and storage footprint of naive LoRA. As it only modifies initialization, LoRAM remains plug-and-play, integrating seamlessly into any pipeline that supports standard LoRA. This is especially valuable for modern large models built on fixed and highly optimized frameworks. In contrast, other initialization methods require costly preprocessing, such as matrix generation [44, 43] or decomposition [40, 42, 41], which complicates adoption in standard workflows.

4 Experiments

We conduct comprehensive experiments to evaluate LoRAM efficiently implemented via the PEFT library [6]. Following conventional settings [40, 41, 35], we assess performance on language tasks and extend the evaluation to vision-language tasks, demonstrating LoRAM's generalization across diverse models and modalities. All experiments are run on servers with 8 NVIDIA H800 GPUs.

Baselines. While extensive research on LoRA has explored aspects like structural modifications and rank control, these directions are largely orthogonal to our focus on hyperparameter analysis within the naive LoRA framework. In line with this, we compare LoRAM with the naive LoRA (ICLR 2022) [7], as well as several representative hyperparameter tuning strategies. We first consider weight-driven initialization (marked "§"), including PiSSA (NeurIPS 2024) [40], which uses the top-r singular vectors and values of pre-trained weights; MiLoRA (NAACL 2025) [41], which utilizes the last r singular vectors and values; and OLoRA [42], which applies orthogonal initialization via QR decomposition. All these methods adopt a fixed scaling factor $\alpha = 1$. We then include RsLoRA [34] (marked "†"), which enhances performance by setting $\alpha = \sqrt{r}$, and LoRA+ (ICML 2024) [35] (marked "‡"), which increases the learning rate with the recommended $\eta_B = 4\eta_A$. We also evaluate data-driven initialization in the ablation study, including LoRA-GA (NeurIPS 2024) [52] and CorDA (NeurIPS 2024) [43], which require extra pipeline to leverage training data information. Most of these baselines have been integrated and validated in the PEFT library.

Table 1: Comparison of LoRAM versus hyperparameter tuning baselines on NLG tasks. Experiments conducted with LLaMA2-7B model using two ranks, reporting mean ± std results (%) over three runs. Bold and underlined values represent the best and second-best performances, respectively.

Rank	#Param	Method	GSM8K	MATH	HumanEval	MBPP	Commonsense
N/A	6738M	Full FT	60.34 ± 1.32	11.74 ± 0.63	32.30 ± 1.26	39.27 ± 1.01	79.20 ± 1.20
16	40M	LoRA	31.51 ± 0.31	4.16 ± 0.27	15.98 ± 0.20	28.65 ± 0.47	66.56 ± 1.21
		RsLoRA†	39.04 ± 0.53	4.94 ± 0.40	18.85 ± 0.66	28.10 ± 0.64	73.24 ± 0.84
		LoRA+‡	31.69 ± 0.64	3.98 ± 0.38	18.54 ± 0.52	28.00 ± 0.81	72.19 ± 1.43
		MiLoRA§	29.70 ± 0.42	4.18 ± 0.21	14.69 ± 0.66	27.23 ± 0.53	67.90 ± 1.20
		OLoRA§	35.83 ± 0.58	4.80 ± 0.53	16.58 ± 0.38	27.44 ± 0.76	73.48 ± 1.09
		PiSSA§	37.68 ± 0.45	5.16 ± 0.41	18.37 ± 0.49	28.62 ± 0.68	73.72 ± 1.05
		LoRAM§	**40.32** ± 0.43	**5.30** ± 0.37	**18.92** ± 0.55	**28.83** ± 0.63	**75.19** ± 1.10
128	320M	LoRA	40.27 ± 0.70	4.72 ± 0.43	20.11 ± 0.32	28.84 ± 0.37	73.64 ± 1.13
		RsLoRA†	50.38 ± 0.37	**7.32** ± 0.28	21.32 ± 0.70	30.73 ± 0.43	77.01 ± 1.17
		LoRA+‡	40.41 ± 0.67	5.28 ± 0.53	20.71 ± 0.88	29.13 ± 0.78	78.19 ± 1.33
		MiLoRA§	39.81 ± 0.89	5.18 ± 0.58	20.39 ± 0.21	29.95 ± 1.05	74.29 ± 1.09
		OLoRA§	50.10 ± 0.64	7.01 ± 0.56	20.72 ± 0.67	30.21 ± 0.89	**78.61** ± 0.97
		PiSSA§	**51.48** ± 0.77	7.04 ± 0.54	21.62 ± 0.48	31.07 ± 0.68	77.28 ± 0.98
		LoRAM§	51.12 ± 0.73	7.25 ± 0.68	**22.03** ± 0.56	**31.53** ± 0.72	77.81 ± 0.96

Table 2: Comparison of LoRAM versus hyperparameter tuning baselines on GLUE benchmark. Experiments conducted with the DeBERTa-v3-base model using rank 8, reporting mean results over three runs. Bold and underlined values represent the best and second-best performances, respectively.

Method	#Param	MNLI	SST-2	MRPC	CoLA	QNLI	QQP	RTE	STS-B
Full FT	184M	88.31	93.57	89.46	67.26	92.80	91.52	83.75	86.87
LoRA	1.33M	90.23	**95.87**	84.06	63.56	93.88	90.55	50.18	87.20
RsLoRA†	1.33M	90.33	95.64	86.38	64.85	93.97	90.26	60.31	88.37
LoRA+‡	1.33M	90.37	95.32	87.54	64.79	**94.32**	90.93	65.37	89.20
MiLoRA§	1.33M	90.28	95.75	87.00	62.58	93.97	90.83	54.87	87.74
OLoRA§	1.33M	90.19	94.83	88.72	**65.59**	93.36	90.74	74.09	88.52
PiSSA§	1.33M	**90.38**	95.64	89.21	65.06	93.84	91.35	74.36	88.90
LoRAM§	1.33M	90.34	95.29	**89.95**	65.53	94.08	**91.70**	**74.72**	**89.93**

4.1 Evaluating the Performance on Natural Language Tasks

Nature Language Generation (NLG). As shown in Table 1, we conduct supervised fine-tuning of LLaMA 2-7B [3] on math, coding, and commonsense reasoning tasks. Our setup strictly follows PiSSA [40], using the AdamW optimizer with a batch size of 128, a learning rate of 2×10^{-5}, a warmup ratio of 0.03, and no weight decay. All experiments are performed on subsets containing 100K data points for one epoch to minimize training overhead. For math tasks, the model is tuned on MetaMathQA [53] and evaluated on GSM8K [54] and MATH [53] validation sets. For coding tasks, we use CodeFeedback [55] as training dataset, with evaluations on HumanEval [56] and MBPP [57]. For commonsense tasks, model is tuned on Commonsense170K [58], and we report averaged accuracy on eight sub-datasets. The results in Table 1 demonstrate that LoRAM consistently outperforms LoRA variants across diverse tasks and rank settings, without requiring matrix decomposition.

Nature Language Understanding (NLU). We evaluate the NLU performance by fine-tuning the DeBERTa-v3-base model [50] with a rank of 8 on eight tasks in the GLUE benchmark [59]. We utilize scripts from the Transformers Library [47] to ensure a fair comparison. All methods are trained with a learning rate of 1×10^{-4} for 3 training epochs, except for MRPC, which uses 5 epochs due to its smaller size. We report overall matched and mismatched accuracy on MNLI, Matthew's correlation on CoLA, Pearson correlation on STS-B, and accuracy on the other datasets. As shown in Table 2, LoRAM achieves competitive performance against PiSSA across most tasks.

4.2 Evaluating the Performance on Vision-Language Tasks

Text-to-image synthesis. We adapt the advanced FLUX.1-12B [51] to address the image customization task, implementing LoRA, PiSSA, and LoRAM under identical configurations: a learning rate of 1×10^{-4}, a batch size of 1 and 1,000 iterations. We set the rank to 8, optimizing 9.3 million

Table 3: Comparing LoRAM with other LoRA variants on LLaVA for multimodel tasks. Bold and underlined values indicate the top and second-best performances, respectively.

Method	MME_{Cog}	MME_{Per}	MMMU	AI2D	ChartQA	OCRBench	TextVQA	ScienceQA
Full FT	280	1541	0.355	0.583	0.251	0.361	0.597	0.722
LoRA	278	1402	0.331	0.557	0.231	0.333	0.536	0.684
RsLoRA[†]	274	1385	0.334	**0.573**	0.227	0.328	0.539	0.694
LoRA+[‡]	283	1389	0.341	0.565	0.229	0.331	0.545	0.690
MiLoRA§	285	1354	0.340	0.564	0.220	0.335	0.536	0.681
OLoRA§	288	1404	0.345	0.565	0.228	0.330	0.540	0.677
PiSSA§	**311**	**1411**	0.344	0.564	0.232	**0.338**	0.547	0.686
LoRAM§	308	1406	**0.350**	0.571	**0.238**	0.336	**0.551**	**0.700**

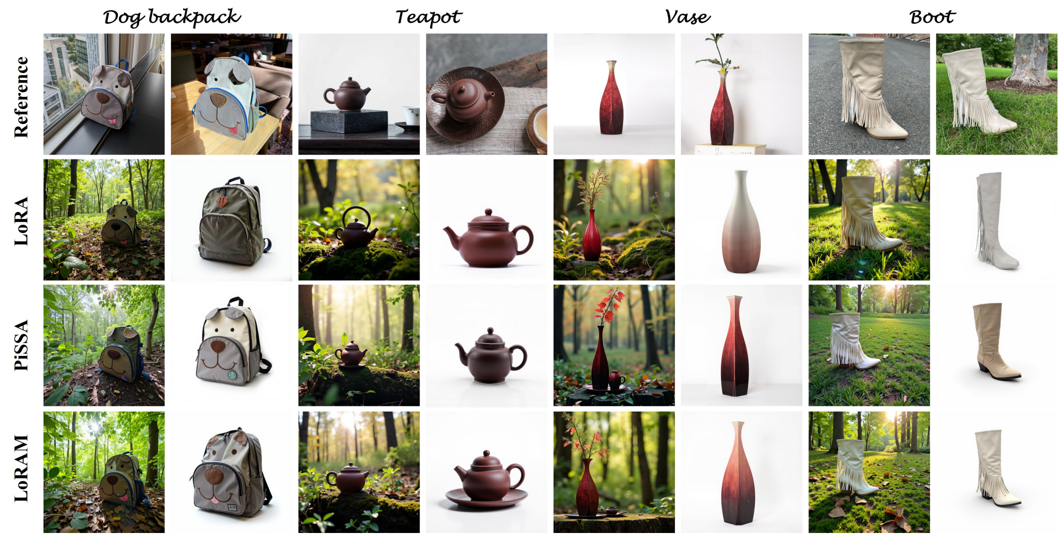

Figure 4: Comparison of LoRA, PiSSA, and LoRAM on image customization task. Experiments conducted with the state-of-the-art FLUX.1-12B model using rank 8.

parameters while maintaining computational efficiency on a single GPU. The training data and prompt template adhere to DreamBooth's protocol [22]. Qualitative results in Figure 4 demonstrate that LoRAM exhibits marginally superior performance in detail fidelity compared to PiSSA.

Image-to-text generation. Following the pipeline of LLaVA [60], we employ CLIP-ViT-L/14 [61] as the visual encoder, Vicuna-13B [62] as the text decoder, and a new visual resampler [63] as the connector. In the pre-training stage, we fine-tune only the perceiver resampler using the CC-595K dataset [60] for one epoch. During the subsequent instruction-tuning stage, we fine-tune both Vicuna and the resampler using a 656K mixture dataset [60]. The learning rate is set to 2×10^{-5}, and the batch size is 128. We follow the official implementation and use a rank of 64. As shown in Table 3, LoRAM achieves favorable performance across multiple multimodal benchmarks.

Training curves. We provide representative training loss curves of diverse initialization methods in Figure 5. It can be noticed that LoRAM is able to have a faster convergence rate in the early stages compared to other LoRA variants and incur smaller losses in the end.

4.3 Ablating the Magnitude Principle in LoRA improvements

We conduct ablation experiments on LLaMA-2-7B [3] under the NLG setting, focusing on the effect of magnitude gain factor, the choice of basis matrix, and the validation of the magnitude principle.

Magnitude Gain Factor. As shown in Table 4, we first evaluate different values of $Q[r]$ and observe that increasing its value slightly improves performance. We further introduce a "tracking mode" that adjusts β in Algorithm 1 based on the initialization magnitudes from reference methods. Specifically, we set $\beta = \sqrt{\frac{\mathbb{V}[B_{\text{ref}} A_{\text{ref}}]}{\mathbb{V}[\Phi_n \Phi_m^\top]}}$, where B_{ref} and A_{ref} are initialization matrix using weight-driven [40, 41] or data-driven approaches [43, 44]. Under this mode, LoRAM essentially matches the performance of prior methods, confirming that magnitudes govern its performance. We also observe that PiSSA,

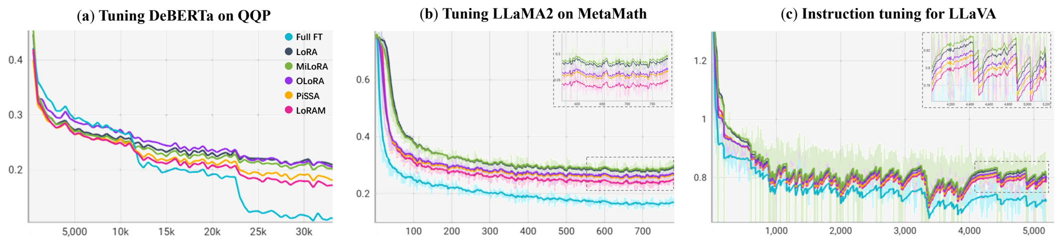

Figure 5: Illustration of training loss curves. LoRAM achieves comparative convergence dynamics to PiSSA across diverse models and benchmarks. See tables and texts for the evaluation results.

Table 4: Results of ablation study. "Orth." denotes the random orthogonal initialization. The left and right sides of the slash indicate the results of the method and the tracking mode, respectively. The average value is calculated over all the ranks and tasks to compare the overall trend of change.

Rank	Task	Q[r]			Basis		Weight-driven		Data-driven		+ RsLoRA	
		$\log \frac{r}{2}$	$\log r^*$	$\log 2r$	Orth.	Gaussian	MiLoRA	PiSSA	CorDA	LoRA-GA	LoRA-GA	LoRAM
16	MATH	5.08	5.30	5.18	4.74	4.62	4.18 / 4.05	5.16 / 5.10	4.60 / 4.14	5.73 / 3.76	7.94	7.22
	GSM8k	40.1	40.3	40.7	36.3	35.8	29.7 / 29.6	37.6 / 36.7	36.2 / 30.7	45.7 / 30.9	51.5	52.1
	MBPP	28.8	28.8	28.3	28.6	27.5	27.2 / 27.8	28.6 / 29.1	25.7 / 28.3	28.3 / 27.8	33.9	31.5
	HumanEval	17.1	18.9	17.1	17.7	17.7	14.6 / 14.7	18.3 / 17.3	15.2 / 15.2	19.5 / 17.7	22.0	18.3
128	MATH	7.52	7.25	7.51	7.40	7.62	5.18 / 5.04	7.04 / 6.95	6.26 / 5.04	9.18 / 7.32	9.08	11.1
	GSM8k	50.7	51.1	50.4	50.2	49.8	39.8 / 39.2	51.4 / 49.5	44.5 / 40.3	54.4 / 50.8	53.6	59.4
	MBPP	31.5	31.5	32.3	31.3	32.8	29.9 / 30.2	31.0 / 29.6	29.6 / 29.9	32.0 / 30.2	31.7	38.1
	HumanEval	20.7	22.0	22.6	23.2	22.6	20.3 / 19.5	21.6 / 20.3	20.1 / 18.9	24.4 / 20.7	26.8	31.7
Average value		25.1	25.5	25.6	24.9	24.8	21.1 / 21.2	25.0 / 24.3	22.7 / 21.6	27.4 / 23.6	29.5	31.1

which selects the top-r singular values, outperforms MiLoRA, which selects the last r singular values. This indicates that leveraging the large dominant singular values enhances performance.

Basis Matrix. We find that the choice of basis matrix generally has limited impact. For instance, replacing the DST basis with a random orthogonal or Gaussian matrix just results in only minor performance degradation. In tracking mode, substituting the SVD-derived basis with DST does not significantly impact performance. A notable exception is LoRA-GA [44], which approximates the full-parameter gradient at initialization. Nonetheless, we emphasize that tracking mode fails not due to incorrectness of magnitude principle, but because the LoRA-GA matrix form maximizes gradient magnitudes of Eq. (2), making it irreplaceable by alternatives and validating magnitude principle[3].

Upper Bound of Magnitude Scaling. While increasing update magnitude generally improves performance, the benefit is not unlimited. For example, applying RsLoRA to LoRA-GA yields a clear gain at rank 8, but the improvement diminishes and may even reverse at rank 128. This suggests that magnitude scaling should be applied conservatively at higher ranks, since larger ranks inherently amplify updates, as demonstrated in our Proposition 2. Given that data-driven methods involve costly gradient and SVD computations, we recommend LoRAM with RsLoRA as a more efficient and scalable alternative for accelerating LoRA convergence and performance.

5 Conclusion

In this paper, we explore the magnitude principle of Low-Rank Adaptation (LoRA) and introduce a novel magnitude-driven initialization strategy, LoRAM, that bridges the gap between efficiency and performance. Our work demystifies the prevailing awareness surrounding spectral initialization methods, demonstrating that their success primarily stems from the amplification of weight update magnitudes. By focusing on magnitude regulation as the key driver of convergence, we provide a unified perspective that connects seemingly disparate hyperparameter adjustments, such as learning rate, scaling factor, and initialization schemes, under a single framework.

Limitations and Future Work. Despite the advancements introduced in this work, several challenges remain open for future research. First, LoRAM mimics spectral initialization magnitudes rather than seeking optimal ones; exploring alternative strategies could yield further gains. Additionally, different layers may benefit from tailored magnitude settings, motivating joint optimization with learning rate and rank. Finally, our work does not explicitly address optimization dynamics and convergence properties. These directions remain valuable for advancing parameter-efficient fine-tuning.

[3]See Proposition 5 in Appendix. We prove LoRA-GA initialization maximizes LoRA gradient magnitude.

References

[1] OpenAI Team. Language models are few-shot learners. In *NeurIPS*, 2020.

[2] OpenAI Team. Gpt-4 technical report. *arXiv preprint arXiv:2303.08774*, 2023.

[3] Meta Team. Llama 2: Open foundation and fine-tuned chat models. *arXiv preprint arXiv:2307.09288*, 2023.

[4] Qwen Team. Qwen technical report. *arXiv preprint arXiv:2309.16609*, 2023.

[5] DeepSeek Team. Deepseek-r1: Incentivizing reasoning capability in llms via reinforcement learning. *arXiv preprint arXiv:2501.12948*, 2025.

[6] S Mangrulkar, S Gugger, L Debut, Yo Belkada, S Paul, and B Bossan. Peft: state-of-the-art parameter-efficient fine-tuning methods. *https://github.com/huggingface/peft*, 2023.

[7] Edward J. Hu, Yelong Shen, Phillip Wallis, Zeyuan Allen-Zhu, Yuanzhi Li, Shean Wang, and Weizhu Chen. Lora: Low-rank adaptation of large language models. In *ICLR*, 2022.

[8] Brian Lester, Rami Al-Rfou, and Noah Constant. The power of scale for parameter-efficient prompt tuning. In *EMNLP*, 2021.

[9] Junxian He, Chunting Zhou, Xuezhe Ma, Taylor Berg-Kirkpatrick, and Graham Neubig. Towards a unified view of parameter-efficient transfer learning. In *ICLR*, 2022.

[10] Ali Edalati, Marzieh S. Tahaei, Ivan Kobyzev, V. Nia, James J. Clark, and Mehdi Rezagholizadeh. Krona: Parameter efficient tuning with kronecker adapter. In *NeurIPS Workshop*, 2023.

[11] Dan Zhang, Tao Feng, Lilong Xue, Yuandong Wang, Yuxiao Dong, and Jie Tang. Parameter-efficient fine-tuning for foundation models. *arXiv preprint arXiv:2501.13787*, 2025.

[12] Sara Babakniya, Ahmed Roushdy Elkordy, Yahya H Ezzeldin, Qingfeng Liu, Kee-Bong Song, Mostafa El-Khamy, and Salman Avestimehr. Slora: Federated parameter efficient fine-tuning of language models. In *NeurIPS Workshop*, 2023.

[13] Yuxuan Yan, Shunpu Tang, Zhiguo Shi, and Qianqian Yang. FeDeRA: Efficient fine-tuning of language models in federated learning leveraging weight decomposition. *arXiv preprint arXiv:2404.18848*, 2024.

[14] Dan Biderman, Jacob Portes, Jose Javier Gonzalez Ortiz, Mansheej Paul, Philip Greengard, Connor Jennings, Daniel King, Sam Havens, Vitaliy Chiley, Jonathan Frankle, et al. Lora learns less and forgets less. *TMLR*, 2024.

[15] Haokun Liu, Derek Tam, Mohammed Muqeeth, Jay Mohta, Tenghao Huang, Mohit Bansal, and Colin A Raffel. Few-shot parameter-efficient fine-tuning is better and cheaper than in-context learning. In *NeurIPS*, 2022.

[16] Ning Ding, Yujia Qin, Guang Yang, Fuchao Wei, Zonghan Yang, Yusheng Su, Shengding Hu, Yulin Chen, Chi-Min Chan, Weize Chen, et al. Parameter-efficient fine-tuning of large-scale pre-trained language models. *Nature Machine Intelligence*, 2023.

[17] Xianghui Sun, Yunjie Ji, Baochang Ma, and Xiangang Li. A comparative study between full-parameter and lora-based fine-tuning on chinese instruction data for instruction following large language model. *arXiv preprint arXiv:2304.08109*, 2023.

[18] Justin Zhao, Timothy Wang, Wael Abid, Geoffrey Angus, Arnav Garg, Jeffery Kinnison, Alex Sherstinsky, Piero Molino, Travis Addair, and Devvret Rishi. Lora land: 310 fine-tuned llms that rival gpt-4, a technical report. *arXiv preprint arXiv:2405.00732*, 2024.

[19] Qinghao Ye, Haiyang Xu, Guohai Xu, Jiabo Ye, Ming Yan, Yiyang Zhou, Junyang Wang, Anwen Hu, Pengcheng Shi, Yaya Shi, et al. mplug-owl: Modularization empowers large language models with multimodality. *arXiv preprint arXiv:2304.14178*, 2023.

[20] Yuwei Guo, Ceyuan Yang, Anyi Rao, Zhengyang Liang, Yaohui Wang, Yu Qiao, Maneesh Agrawala, Dahua Lin, and Bo Dai. Animatediff: Animate your personalized text-to-image diffusion models without specific tuning. In *ICLR*, 2024.

[21] Andreas Blattmann, Tim Dockhorn, Sumith Kulal, Daniel Mendelevitch, Maciej Kilian, Dominik Lorenz, Yam Levi, Zion English, Vikram Voleti, Adam Letts, et al. Stable video diffusion: Scaling latent video diffusion models to large datasets. *arXiv preprint arXiv:2311.15127*, 2023.

[22] Nataniel Ruiz, Yuanzhen Li, Varun Jampani, Yael Pritch, Michael Rubinstein, and Kfir Aberman. Dreambooth: Fine tuning text-to-image diffusion models for subject-driven generation. In *CVPR*, 2023.

[23] Nam Hyeon-Woo, Moon Ye-Bin, and Tae-Hyun Oh. Fedpara: Low-rank hadamard product for communication-efficient federated learning. In *ICLR*, 2022.

[24] Bojia Zi, Xianbiao Qi, Lingzhi Wang, Jianan Wang, Kam-Fai Wong, and Lei Zhang. Delta-lora: Fine-tuning high-rank parameters with the delta of low-rank matrices. *arXiv preprint arXiv:2309.02411*, 2022.

[25] Ziqi Gao, Qichao Wang, Aochuan Chen, Zijing Liu, Bingzhe Wu, Liang Chen, and Jia Li. Parameter-efficient fine-tuning with discrete fourier transform. In *ICML*, 2022.

[26] Ting Jiang, Shaohan Huang, Shengyue Luo, Zihan Zhang, Haizhen Huang, Furu Wei, Weiwei Deng, Feng Sun, Qi Zhang, Deqing Wang, et al. Mora: High-rank updating for parameter-efficient fine-tuning. *arXiv preprint arXiv:2405.12130*, 2024.

[27] Vladislav Lialin, Sherin Muckatira, Namrata Shivagunde, and Anna Rumshisky. Relora: High-rank training through low-rank updates. In *ICLR*, 2024.

[28] Wenhan Xia, Chengwei Qin, and Elad Hazan. Chain of lora: Efficient fine-tuning of language models via residual learning. In *ICML*, 2024.

[29] Xiangdi Meng, Damai Dai, Weiyao Luo, Zhe Yang, Shaoxiang Wu, Xiaochen Wang, Peiyi Wang, Qingxiu Dong, Liang Chen, and Zhifang Sui. Periodiclora: Breaking the low-rank bottleneck in lora optimization. *arXiv preprint arXiv.2402.16141*, 2024.

[30] Bingcong Li, Liang Zhang, Aryan Mokhtari, and Niao He. On the crucial role of initialization for matrix factorization. In *ICLR*, 2025.

[31] Yuchen Zeng and Kangwook Lee. The expressive power of low-rank adaptation. In *ICLR*, 2024.

[32] Qingru Zhang, Minshuo Chen, Alexander W. Bukharin, Pengcheng He, Yu Cheng, Weizhu Chen, and Tuo Zhao. Adaptive budget allocation for parameter-efficient fine-tuning. In *ICLR*, 2023.

[33] Ning Ding, Xingtai Lv, Qiaosen Wang, Yulin Chen, Bowen Zhou, Zhiyuan Liu, and Maosong Sun. Sparse low-rank adaptation of pre-trained language models. In *EMNLP*, 2023.

[34] Damjan Kalajdzievski. A rank stabilization scaling factor for fine-tuning with lora. *arXiv preprint arXiv:2312.03732*, 2023.

[35] Soufiane Hayou, Nikhil Ghosh, and Bin Yu. Lora+: Efficient low rank adaptation of large models. In *ICML*, 2024.

[36] Jiacheng Zhu, Kristjan Greenewald, Kimia Nadjahi, Haitz Sáez de Ocáriz Borde, Rickard Brüel Gabrielsson, Leshem Choshen, Marzyeh Ghassemi, Mikhail Yurochkin, and Justin Solomon. Asymmetry in low-rank adapters of foundation models. In *ICML*, 2024.

[37] Soufiane Hayou, Nikhil Ghosh, and Bin Yu. The impact of initialization on lora finetuning dynamics. In *NeurIPS*, 2024.

[38] Fangzhao Zhang and Mert Pilanci. Riemannian preconditioned lora for fine-tuning foundation models. In *ICML*, 2024.

[39] Yuanhe Zhang, Fanghui Liu, and Yudong Chen. One-step full gradient suffices for low-rank fine-tuning, provably and efficiently. *arXiv preprint arXiv:2502.01235*, 2025.

[40] Fanxu Meng, Zhaohui Wang, and Muhan Zhang. Pissa: Principal singular values and singular vectors adaptation of large language models. In *NeurIPS*, 2024.

[41] Hanqing Wang, Zeguan Xiao, Yixia Li, Shuo Wang, Guanhua Chen, and Yun Chen. Milora: Harnessing minor singular components for parameter-efficient llm finetuning. In *NAACL*, 2025.

[42] Kerim Büyükakyüz. Olora: Orthonormal low-rank adaptation of large language models. *arXiv preprint arXiv:2406.01775*, 2024.

[43] Yibo Yang, Xiaojie Li, Zhongzhu Zhou, Shuaiwen Leon Song, Jianlong Wu, Liqiang Nie, and Bernard Ghanem. Corda: Context-oriented decomposition adaptation of large language models. In *NeurIPS*, 2024.

[44] Shaowen Wang, Linxi Yu, and Jian Li. Lora-ga: Low-rank adaptation with gradient approximation. In *NeurIPS*, 2024.

[45] Dawid Jan Kopiczko, Tijmen Blankevoort, and Yuki Markus Asano. Vera: Vector-based random matrix adaptation. In *ICLR*, 2024.

[46] Tim Dettmers, Artidoro Pagnoni, Ari Holtzman, and Luke Zettlemoyer. Qlora: Efficient finetuning of quantized llms. In *NeurIPS*, 2023.

[47] HuggingFace Team. Transformers: State-of-the-art natural language processing. In *EMNLP*, 2020.

[48] Yuren Mao, Yuhang Ge, Yijiang Fan, Wenyi Xu, Yu Mi, Zhonghao Hu, and Yunjun Gao. A survey on lora of large language models. *Frontiers of Computer Science*, 2025.

[49] Kaiming He, Xiangyu Zhang, Shaoqing Ren, and Jian Sun. Delving deep into rectifiers: Surpassing human-level performance on imagenet classification. In *ICCV*, 2015.

[50] Pengcheng He, Jianfeng Gao, and Weizhu Chen. Debertav3: Improving deberta using electra-style pre-training with gradient-disentangled embedding sharing. In *ICLR*, 2023.

[51] Black Forest Labs. Flux. *https://github.com/black-forest-labs/flux*, 2024.

[52] Zhengbo Wang, Jian Liang, Ran He, Zilei Wang, and Tieniu Tan. Lora-pro: Are low-rank adapters properly optimized? In *ICLR*, 2025.

[53] Longhui Yu, Weisen Jiang, Han Shi, Jincheng Yu, Zhengying Liu, Yu Zhang, James T Kwok, Zhenguo Li, Adrian Weller, and Weiyang Liu. Metamath: Bootstrap your own mathematical questions for large language models. In *ICLR*, 2024.

[54] Karl Cobbe, Vineet Kosaraju, Mohammad Bavarian, Mark Chen, Heewoo Jun, Lukasz Kaiser, Matthias Plappert, Jerry Tworek, Jacob Hilton, Reiichiro Nakano, Christopher Hesse, and John Schulman. Training verifiers to solve math word problems. *arXiv preprint arXiv:2110.14168*, 2021.

[55] Tianyu Zheng, Ge Zhang, Tianhao Shen, Xueling Liu, Bill Yuchen Lin, Jie Fu, Wenhu Chen, and Xiang Yue. Opencodeinterpreter: Integrating code generation with execution and refinement. *arXiv preprint arXiv:2402.14658*, 2024.

[56] Qinkai Zheng, Xiao Xia, Xu Zou, Yuxiao Dong, Shan Wang, Yufei Xue, Zihan Wang, Lei Shen, Andi Wang, Yang Li, et al. Codegeex: A pre-trained model for code generation with multilingual evaluations on humaneval-x. In *KDD*, 2023.

[57] Jacob Austin, Augustus Odena, Maxwell Nye, Maarten Bosma, Henryk Michalewski, David Dohan, Ellen Jiang, Carrie Cai, Michael Terry, Quoc Le, et al. Program synthesis with large language models. *arXiv preprint arXiv:2108.07732*, 2021.

[58] Zhiqiang Hu, Lei Wang, Yihuai Lan, Wanyu Xu, Ee-Peng Lim, Lidong Bing, Xing Xu, Soujanya Poria, and Roy Lee. LLM-adapters: An adapter family for parameter-efficient fine-tuning of large language models. In *EMNLP*, 2023.

[59] Alex Wang, Amanpreet Singh, Julian Michael, Felix Hill, Omer Levy, and Samuel R. Bowman. Glue: A multi-task benchmark and analysis platform for natural language understanding. In *EMNLP Workshop*, 2018.

[60] Haotian Liu, Chunyuan Li, Yuheng Li, and Yong Jae Lee. Improved baselines with visual instruction tuning. In *CVPR*, 2024.

[61] Alec Radford, Jong Wook Kim, Chris Hallacy, Aditya Ramesh, Gabriel Goh, Sandhini Agarwal, Girish Sastry, Amanda Askell, Pamela Mishkin, Jack Clark, et al. Learning transferable visual models from natural language supervision. In *ICML*, 2021.

[62] Lianmin Zheng, Wei-Lin Chiang, Ying Sheng, Siyuan Zhuang, Zhanghao Wu, Yonghao Zhuang, Zi Lin, Zhuohan Li, Dacheng Li, Eric Xing, et al. Judging llm-as-a-judge with mt-bench and chatbot arena. In *NeurIPS*, 2024.

[63] Zonghao Guo, Ruyi Xu, Yuan Yao, Junbo Cui, Zanlin Ni, Chunjiang Ge, Tat-Seng Chua, Zhiyuan Liu, and Gao Huang. Llava-uhd: an lmm perceiving any aspect ratio and high-resolution images. In *ECCV*, 2024.

[64] Tero Karras, Samuli Laine, Miika Aittala, Janne Hellsten, Jaakko Lehtinen, and Timo Aila. Analyzing and improving the image quality of stylegan. In *CVPR*, 2020.

[65] Robin Rombach, Andreas Blattmann, Dominik Lorenz, Patrick Esser, and Björn Ommer. High-resolution image synthesis with latent diffusion models. In *CVPR*, 2022.

[66] Zicheng Zhang, Yinglu Liu, Congying Han, Tiande Guo, Ting Yao, and Tao Mei. Generalized one-shot domain adaptation of generative adversarial networks. In *NeurIPS*, 2022.

[67] Zicheng Zhang, Bonan Li, Xuecheng Nie, Congying Han, Tiande Guo, and Luoqi Liu. Towards consistent video editing with text-to-image diffusion models. In *NeurIPS*, 2023.

[68] Bonan Li, Zicheng Zhang, Songhua Liu, Weihao Yu, Xinchao Wang, et al. Top-down compression: Revisit efficient vision token projection for visual instruction tuning. *arXiv preprint arXiv:2505.11945*, 2025.

[69] Ai Han, Junxing Hu, Pu Wei, Zhiqian Zhang, Yuhang Guo, Jiawei Lu, and Zicheng Zhang. Joyagents-r1: Joint evolution dynamics for versatile multi-llm agents with reinforcement learning. *arXiv preprint arXiv:2506.19846*, 2025.

[70] Menglin Yang, Jialin Chen, Yifei Zhang, Jiahong Liu, Jiasheng Zhang, Qiyao Ma, Harshit Verma, Qianru Zhang, Min Zhou, Irwin King, et al. Low-rank adaptation for foundation models: A comprehensive review. *arXiv preprint arXiv:2501.00365*, 2024.

[71] Pengjie Ren, Chengshun Shi, Shiguang Wu, Mengqi Zhang, Zhaochun Ren, Maarten de Rijke, Zhumin Chen, and Jiahuan Pei. Mini-ensemble low-rank adapters for parameter-efficient fine-tuning. In *ACL*, 2024.

[72] Yinqiao Li, Linqi Song, and Hanxu Hou. Loran: Improved low-rank adaptation by a non-linear transformation. In *EMNLP Findings*, 2024.

[73] Yibo Zhong, Haoxiang Jiang, Lincan Li, Ryumei Nakada, Tianci Liu, Linjun Zhang, Huaxiu Yao, and Haoyu Wang. Neat: Nonlinear parameter-efficient adaptation of pre-trained models. *arXiv preprint arXiv:2410.01870*, 2024.

[74] Yeming Wen and Swarat Chaudhuri. Batched low-rank adaptation of foundation models. In *ICLR*, 2024.

[75] Shih-Yang Liu, Chien-Yi Wang, Hongxu Yin, Pavlo Molchanov, Yu-Chiang Frank Wang, Kwang-Ting Cheng, and Min-Hung Chen. Dora: Weight-decomposed low-rank adaptation. In *ICML*, 2024.

[76] Sebastian Raschka. Practical tips for finetuning llms using lora. `https://magazine.sebastianraschka.com/p/practical-tips-for-finetuning-llms`, 2023.

[77] Yang Lin, Xinyu Ma, Xu Chu, Yujie Jin, Zhibang Yang, Yasha Wang, and Hong Mei. Lora dropout as a sparsity regularizer for overfitting control. *arXiv preprint arXiv:2404.09610*, 2024.

[78] Longteng Zhang, Lin Zhang, Shaohuai Shi, Xiaowen Chu, and Bo Li. Lora-fa: Memory-efficient low-rank adaptation for large language models fine-tuning. *arXiv preprint arXiv:2308.03303*, 2023.

[79] Klaudia Bałazy, Mohammadreza Banaei, Karl Aberer, and Jacek Tabor. Lora-xs: Low-rank adaptation with extremely small number of parameters. *arXiv preprint arXiv:2405.17604*, 2024.

[80] Yixiao Li, Yifan Yu, Chen Liang, Pengcheng He, Nikos Karampatziakis, Weizhu Chen, and Tuo Zhao. Loftq: Lora-fine-tuning-aware quantization for large language models. In *ICLR*, 2024.

[81] Xavier Glorot and Yoshua Bengio. Understanding the difficulty of training deep feedforward neural networks. In *AISTATS*, 2010.

[82] Fabian Paischer, Lukas Hauzenberger, Thomas Schmied, Benedikt Alkin, Marc Peter Deisenroth, and Sepp Hochreiter. One initialization to rule them all: Fine-tuning via explained variance adaptation. *arXiv preprint arXiv:2410.07170*, 2024.

[83] Uijeong Jang, Jason D. Lee, and Ernest K. Ryu. Lora training in the NTK regime has no spurious local minima. In *ICML*, 2024.

[84] Sadhika Malladi, Alexander Wettig, Dingli Yu, Danqi Chen, and Sanjeev Arora. A kernel-based view of language model fine-tuning. In *ICML*, 2023.

A Related Work

Advances in Low-Rank Adaptation. The growing scale [1, 2, 3, 4, 64, 65] of large pre-trained models across various domains urgently demands efficient fine-tuning methods [18, 19, 20, 21, 22, 66, 67, 68, 69]. LoRA [7] has garnered significant attention in leveraging low-rank structures to represent weight updates, with subsequent studies expanding its foundations and applications [70, 48]. Existing improvements to LoRA primarily focus on three directions:

• The low-rank constraint creates bottlenecks when learning complex features. Recent approaches enhance expressiveness through iterative stacking of LoRA modules [27, 28, 24, 29], high-order matrix operations [23, 10], and customized architectural designs [71, 26, 72, 73, 74, 32, 75].

• The non-convex landscapes pose challenges for numerical optimization and hyperparameter tuning [30]. Researchers have explored to improve scaling factor [34, 76, 14], learning rate [35], dropout rate [77], optimizers [30, 38, 39, 44], and initialization strategies [40, 41, 42, 37, 39, 43, 44].

• Recent works reduce computational and memory overhead through freezing parameters [78, 36], designing more compact adapters [45, 79, 25] and parameter quantization [40, 46, 80].

Knowledge-Driven Low-Rank Initialization. Proper initialization critically influences neural network training outcomes [81, 49]. The standard LoRA [7] initializes its low-rank matrices with random noise and zeros, referred to as "Noise & Zero" scheme, demonstrated to hinder convergence. Recent advances address this limitation by leveraging knowledge from pre-trained weights [40, 41, 42, 12] or task-specific data [39, 43, 44]. Most prominent approaches involve Singular Value Decomposition (SVD), which allows flexible control over matrix rank. As a pioneer, PiSSA [40] initializes LoRA weights using principal singular components of pre-trained matrices, aligning adaptation directions with the most significant parameter variations to accelerate convergence. Subsequent works [43, 44, 39, 82] propose data-driven strategies that incorporate domain knowledge into adapter construction. For instance, LoRA-GA [44] aligns low-rank gradient directions with full fine-tuning counterparts during initialization. While these methods boost performance and retain the core LoRA structure, their theoretical effects on optimization dynamics remain unclear. More importantly, they are less pluggable than LoRA, requiring extra computational pipelines and storage for SVD buffers.

Optimization Dynamics of LoRA. LoRA exhibits inherently nonlinear and non-convex optimization dynamics that complicate theoretical analysis [30]. Most existing theoretical studies are limited to simplified and idealized scenarios, such as the lazy-training regime [83, 84] and infinite-width limit[35, 37]. A common goal across existing studies involves ensuring feature learning stability to prevent unstable or collapsed training dynamics. For instance, [34] proves that improper scaling factors induce gradient collapse in high-rank adapters, proposing modified scaling mechanisms to stabilize forward and backward propagation. Recent work [35, 36, 37] reveals critical asymmetries in LoRA: The two low-rank matrices exhibit divergent distinct impacts on optimization trajectories. This asymmetry motivates [35] to employ distinct learning rates for each matrix. For SVD-based initialization, [39] investigates principal components derived from single-step full fine-tuning gradients [44], providing convergence guarantees yet under restrictive assumptions. Moreover, such analyses still fail to explain the efficacy of alternative approaches like weight-driven initialization [40].

The intricate nature of LoRA and its numerous advancements motivates us to seek a streamlined principle explaining its empirical success and guiding practical applications. We identify update magnitude amplification as a key mechanism, unifying seemingly disparate elements, such as scaling factors [34, 14], initialization strategies [40, 44], and learning rates [35], into a cohesive perspective.

B Lower Bound on Representation Error

Proposition 1 (Lower Bound on Representation Error). *Consider the function class of LoRA-parameterized linear models:*

$$\mathcal{H} = \left\{ (W + \alpha BA)x \mid B \in \mathbb{R}^{n\times r}, A \in \mathbb{R}^{r\times m}, \nu[A] \leq M_1, \nu[B] \leq M_2 \right\}.$$

Let $R(f) = \mathbb{E}_{(x,y)\sim\mathcal{D}}[\ell(f(x), y)]$ *denote the expected regression loss under data distribution* $\mathcal{D}$*, with squared error loss* $\ell(f(x), y) = \|y - f(x)\|^2$*. Define* $f^* = \arg\min_f R(f)$ *as the globally optimal predictor and* $f^*_{\mathcal{H}} = \arg\min_{f\in\mathcal{H}} R(f)$ *as the optimal predictor within* $\mathcal{H}$*. With loss of generality, we consider the optimal predictor is linear, i.e.,* $f^*(x) = W^*x$*. Assume that the input covariance matrix is positive definite, i.e.,* $\Sigma_{\mathcal{D}} = \mathbb{E}_{x\sim\mathcal{D}}[xx^\top] \succ 0$*, and the magnitudes is limited,* *satisfying* $\alpha r\sqrt{mnM_1M_2} < \|W^* - W_0\|_F$*. Then, the representation error is strictly positive and lower bounded:*

$$R(f^*_{\mathcal{H}}) - R(f^*) \geq \lambda_{\min}(\Sigma_{\mathcal{D}})\left(\|W^* - W_0\|_F - \alpha r\sqrt{mnM_1M_2}\right)^2 > 0,$$

where $\lambda_{\min}(\cdot)$ *denotes the smallest eigenvalue of the matrix.*

Proof. Due to the linear learnability, we have that $y(x) = f^*(x) = W^*x$. For any W, we have that

$$\begin{aligned} R(W) &= \mathbb{E}_{x\sim\mathcal{D}}\left[\|(W - W^*)x\|^2\right] \\ &= \mathbb{E}_{x\sim\mathcal{D}}\left[(W - W^*)x\left((W - W^*)x\right)^\top\right] \\ &= \mathrm{Tr}\left((W - W^*)\Sigma_{\mathcal{D}}(W - W^*)^\top\right) \\ &\geq \lambda_{\min}(\Sigma_{\mathcal{D}})\|W - W^*\|_F^2. \end{aligned} \tag{13}$$

The last inequality comes from $\lambda_{\min}(\Sigma_{\mathcal{D}}) > 0$.

Due to $\nu[A] \leq M_1, \nu[B] \leq M_2$, we have that

$$\|A\|_F^2 \leq rmM_1,\ \|B\|_F^2 \leq rnM_2.$$

Further, for any $A,\ B \in \mathcal{H}$, we have that

$$\begin{aligned} \|W_0 + \alpha BA - W^*\|_F &\geq \|W_0 - W^*\|_F - \|\alpha BA\|_F \\ &\geq \|W_0 - W^*\|_F - \alpha\|A\|_F\|B\|_F \\ &\geq \|W_0 - W^*\|_F - \alpha r\sqrt{mnM_1M_2} \\ &> 0. \end{aligned} \tag{14}$$

Therefore, we have that

$$\begin{aligned} &R(f^*_{\mathcal{H}}) - R(f^*) \\ =& \min_{\nu[A]\leq M_1, \nu[B]\leq M_2} R(W_0 + \alpha BA) \\ \geq& \lambda_{\min}(\Sigma_{\mathcal{D}}) \min_{\nu[A]\leq M_1, \nu[B]\leq M_2} \|W_0 + \alpha BA - W^*\|_F^2 \\ \geq& \lambda_{\min}(\Sigma_{\mathcal{D}})\left(\|W_0 - W^*\|_F - \alpha r\sqrt{mnM_1M_2}\right)^2 > 0. \end{aligned}$$

The first inequality comes from Eq. (13) and the last inequality comes from Eq. (14). □

C Proof of Main Theorems

C.1 Proof of Parameter Scaling Equivalence

Proposition 2 (Parameter Scaling Equivalence)**.** *For LoRA layers defined in Eq.* (1)*, consider decomposing the scaling factor* $\alpha = \alpha'\alpha_A\alpha_B$*, where* $\alpha', \alpha_A, \alpha_B \in \mathbb{R}^+$*. Under the commonly used optimization frameworks with negligible numerical errors, the following parametrization schemes exhibit dynamical equivalence throughout training: For all iterations* $t \geq 0$*,* $\Delta W^{(t)}_{\mathrm{LoRA}} = \Delta\tilde{W}^{(t)}_{\mathrm{LoRA}}$ *and* $W^{(t)}_{\mathrm{LoRA}} = \tilde{W}^{(t)}_{\mathrm{LoRA}}$*, where* $\tilde{A}^{(t)}$*,* $\tilde{B}^{(t)}$ *and* $\tilde{W}^{(t)}$ *represent the re-parameterized versions.*

	Original	*SGD*	*Adam*
Representation	αBAx	$\alpha'\tilde{B}\tilde{A}x$	$\alpha'\tilde{B}\tilde{A}x$
Initialization	$A^{(0)} = A_{init}, B^{(0)} = B_{init}$	$\tilde{A}^{(0)} = \alpha_A A_{init}, \tilde{B}^{(0)} = \alpha_B B_{init}$	$\tilde{A}^{(0)} = \alpha_A A_{init}, \tilde{B}^{(0)} = \alpha_B B_{init}$
Learning Rates	$\eta_A > 0, \eta_B > 0$	$\eta_{\tilde{A}} = \alpha_A^2\eta_A, \eta_{\tilde{B}} = \alpha_B^2\eta_B$	$\eta_{\tilde{A}} = \alpha_A\eta_A, \eta_{\tilde{B}} = \alpha_B\eta_B$

Proof. Given LoRA's weight decomposition $W_{\mathrm{LoRA}} = \alpha BA$ where $\alpha > 0$, the gradient updates follow:

$$\Delta W^{(t)}_{\mathrm{LoRA}} = \alpha(B^{(t+1)}A^{(t+1)} - B^{(t)}A^{(t)}), \tag{15}$$

with learning rates η_A, η_B for parameters A and B, respectively. We define reparameterized parameters $\tilde{A} = \alpha_A A$, $\tilde{B} = \alpha_B B$, and $\alpha' = \alpha/(\alpha_A\alpha_B)$. The LoRA projection becomes:

$$W_{\mathrm{LoRA}} = \alpha BA = \alpha'\tilde{B}\tilde{A}. \tag{16}$$

This transformation preserves the functional form while redistributing scaling factors.

Proof for SGD Under initial conditions:

$$\tilde{A}^{(0)} = \alpha_A A_{\text{init}}, \tag{17}$$
$$\tilde{B}^{(0)} = \alpha_B B_{\text{init}}. \tag{18}$$

Gradients for reparameterized parameters:

$$\nabla_{\tilde{A}} L = \alpha' \tilde{B}^\top \nabla_W L, \tag{19}$$
$$\nabla_{\tilde{B}} L = \alpha' \nabla_W L \tilde{A}^\top. \tag{20}$$

With learning rates $\eta_{\tilde{A}} = \alpha_A^2 \eta_A$, $\eta_{\tilde{B}} = \alpha_B^2 \eta_B$ and $t = 0$:

$$\begin{aligned}
\tilde{A}^{(t+1)} &= \tilde{A}^{(t)} - \alpha_A^2 \eta_A \nabla_{\tilde{A}} L^{(t)} & (21)\\
&= \alpha_A A^{(t)} - \alpha_A^2 \eta_A (\alpha' \alpha_B B^{(t)})^\top \nabla_W L^{(t)} & (22)\\
&= \alpha_A \left(A^{(t)} - \alpha \eta_A (B^{(t)})^\top \nabla_W L^{(t)} \right) & (23)\\
&= \alpha_A \left(A^{(t)} - \eta_A \nabla_A L^{(t)} \right) & (24)\\
&= \alpha_A A^{(t+1)}. & (25)
\end{aligned}$$

Similarly for $\tilde{B}$:

$$\tilde{B}^{(t+1)} = \alpha_B \left(B^{(t)} - \eta_B \nabla_B L^{(t)} \right) = \alpha_B B^{(t+1)}. \tag{26}$$

These equations propagate through all $t > 0$ via mathematical induction. Compare weight increments:

$$\begin{aligned}
\Delta \tilde{W}_{\text{LoRA}}^{(t)} &= \alpha' [\tilde{B}^{(t+1)} \tilde{A}^{(t+1)} - \tilde{B}^{(t)} \tilde{A}^{(t)}] & (27)\\
&= \alpha' \alpha_A \alpha_B [B^{(t+1)} A^{(t+1)} - B^{(t)} A^{(t)}] & (28)\\
&= \alpha [B^{(t+1)} A^{(t+1)} - B^{(t)} A^{(t)}] & (29)\\
&= \Delta W_{\text{LoRA}}^{(t)}. & (30)
\end{aligned}$$

Proof for Adam Adam maintains exponential moving averages (m_t, v_t) for gradients. Under parameter scaling $\tilde{P} = kP$, gradients transform as $\nabla_{\tilde{P}} L = k \nabla_P L$. The momentum terms inherit scaling factors:

$$m_{\tilde{P}} = \beta_1 m_{\tilde{P}} + (1 - \beta_1) k \nabla_P L, \tag{31}$$
$$v_{\tilde{P}} = \beta_2 v_{\tilde{P}} + (1 - \beta_2) k^2 (\nabla_P L)^2. \tag{32}$$

The pratical gradients for Adam:

$$\begin{aligned}
\nabla^\dagger \tilde{P} &= m_{\tilde{P}} / \sqrt{v_{\tilde{P}} + \epsilon} & (33)\\
&= [\beta_1 m_P + ...] / \sqrt{\beta_2 v_P + ...} & (34)
\end{aligned}$$

When setting $\epsilon = 0$ for alleviating numerical errors, we have $\nabla^\dagger \tilde{P} = \nabla^\dagger P$. Setting $\eta_{\tilde{P}} = k \eta_P$ cancels scaling factors, preserving update magnitudes. With learning rates $\eta_{\tilde{A}} = \alpha_A \eta_A$, $\eta_{\tilde{B}} = \alpha_B \eta_B$ and $t = 0$:

$$\begin{aligned}
\tilde{A}^{(t+1)} &= \tilde{A}^{(t)} - \alpha_A \eta_A \nabla_{\tilde{A}}^\dagger L^{(t)} & (35)\\
&= \alpha_A A^{(t)} - \alpha_A \eta_A \nabla_A^\dagger L^{(t)} & (36)\\
&= \alpha_A A^{(t+1)}. & (37)
\end{aligned}$$

Similarly for $\tilde{B}$. These equalities propagate through all $t > 0$ via mathematical induction.

□

C.2 Proof of Proposition 2

For the convenience, we split the proof of Proposition 2 into two parts.

Proposition 3 (Parameter Magnitude Dynamics)**.** *Consider LoRA parameters $A^{(t)}$ and $B^{(t)}$ updated with learning rate η. Assume: $A^{(0)} \sim \mathcal{N}(\mathbf{0}, \sigma_A^2 I)$, $B^{(0)} \sim \mathcal{N}(\mathbf{0}, \sigma_B^2 I)$, $\nabla_W L \sim \mathcal{N}(\mathbf{0}, \sigma_L^2 I)$, and $\mathbb{E}[\langle A^{(t)}, \nabla_A L^{(t)} \rangle] = \mathbb{E}[\langle B^{(t)}, \nabla_B L^{(t)} \rangle] = 0$. Under these conditions, the parameter norm vector $\boldsymbol{e}_t = \left[\mathbb{E}[\|A^{(t)}\|_F^2], \mathbb{E}[\|B^{(t)}\|_F^2]\right]^T$ evolve as the following linear dynamical system (left) with closed-form solution (right):*

$$\boldsymbol{e}_{t+1} = \left(I + \begin{bmatrix} 0 & \gamma_A \\ \gamma_B & 0 \end{bmatrix}\right) \boldsymbol{e}_t, \quad \boldsymbol{e}_t = \begin{bmatrix} \frac{\lambda_+^t + \lambda_-^t}{2} & \sqrt{\frac{\gamma_A}{\gamma_B}} \frac{\lambda_+^t - \lambda_-^t}{2} \\ \sqrt{\frac{\gamma_B}{\gamma_A}} \frac{\lambda_+^t - \lambda_-^t}{2} & \frac{\lambda_+^t + \lambda_-^t}{2} \end{bmatrix} \boldsymbol{e}_0. \tag{38}$$

where $\gamma_A = m\eta^2\sigma_L^2$, $\gamma_B = n\eta^2\sigma_L^2$ and $\lambda_\pm = 1 \pm \sqrt{\gamma_A \gamma_B}$. Similarly, the parameter magnitudes $\boldsymbol{\nu}_t = \left[\mathbb{E}[\nu[A^{(t)}]], \mathbb{E}[\nu[B^{(t)}]]\right]^T$ evolve as a linear dynamical system:

$$\boldsymbol{\nu}_t = \left(I + \begin{bmatrix} 0 & \gamma_B \\ \gamma_A & 0 \end{bmatrix}\right) \boldsymbol{\nu}_{t-1}. \tag{39}$$

Proof. Following the gradient descent update rule, the parameter dynamics are:

$$\begin{cases} A_{t+1} = A_t - \eta \nabla_A L_t \\ B_{t+1} = B_t - \eta \nabla_B L_t \end{cases}, \tag{40}$$

where the gradient relationships $\nabla_A L = B^\top (\nabla_W L)$ and $\nabla_B L = (\nabla_W L) A^\top$ are derived from the LoRA architecture. Expand the Frobenius norm for A_{t+1}:

$$\|A_{t+1}\|_F^2 = \|A_t\|_F^2 - 2\eta \langle A_t, \nabla_A L_t \rangle + \eta^2 \|\nabla_A L_t\|_F^2. \tag{41}$$

Taking expectations (using independence $\mathbb{E}[\langle A_t, \nabla_A L_t \rangle] = 0$):

$$\mathbb{E}\|A_{t+1}\|_F^2 = \mathbb{E}\|A_t\|_F^2 + \eta^2 \mathbb{E}\|\nabla_A L_t\|_F^2. \tag{42}$$

Similarly, for B_{t+1}:

$$\mathbb{E}\|B_{t+1}\|_F^2 = \mathbb{E}\|B_t\|_F^2 + \eta^2 \mathbb{E}\|\nabla_B L_t\|_F^2. \tag{43}$$

Expand the norm of $\nabla_A L = B^\top (\nabla_W L)$:

$$\|\nabla_A L\|_F^2 = \text{Tr}((\nabla_A L)(\nabla_A L)^\top) = \text{Tr}(B^\top (\nabla_W L)(\nabla_W L)^\top B). \tag{44}$$

Taking expectations (using gradient entry independence):

$$\mathbb{E}\|\nabla_A L\|_F^2 = \text{Tr}\left(B^\top \mathbb{E}[(\nabla_W L)(\nabla_W L)^\top] B\right) = m\sigma_L^2 \|B\|_F^2. \tag{45}$$

where $\mathbb{E}[(\nabla_W L)(\nabla_W L)^\top] = m\sigma_L^2 I_n$ follows from the i.i.d. assumption on gradient entries.

For $\nabla_B L = (\nabla_W L) A^\top$:

$$\mathbb{E}\|\nabla_B L\|_F^2 = \text{Tr}\left(A \mathbb{E}[(\nabla_W L)^\top (\nabla_W L)] A^\top\right) = n\sigma_L^2 \|A\|_F^2. \tag{46}$$

Substitute gradient norms results:

$$\begin{cases} \mathbb{E}\|A_{t+1}\|_F^2 = \mathbb{E}\|A_t\|_F^2 + \eta^2 m\sigma_L^2 \mathbb{E}\|B_t\|_F^2 \\ \mathbb{E}\|B_{t+1}\|_F^2 = \mathbb{E}\|B_t\|_F^2 + \eta^2 n\sigma_L^2 \mathbb{E}\|A_t\|_F^2 \end{cases}. \tag{47}$$

Define parameters and state vector:

$$\gamma_A = \eta^2 m\sigma_L^2, \quad \gamma_B = \eta^2 n\sigma_L^2, \quad \mathbf{e}_t = \begin{bmatrix} \mathbb{E}\|A_t\|_F^2 \\ \mathbb{E}\|B_t\|_F^2 \end{bmatrix}. \tag{48}$$

The recursive system becomes:

$$\boldsymbol{e}_{t+1} = \begin{bmatrix} 1 & \gamma_A \\ \gamma_B & 1 \end{bmatrix} \boldsymbol{e}_t = \left(I + \begin{bmatrix} 0 & \gamma_A \\ \gamma_B & 0 \end{bmatrix}\right) \boldsymbol{e}_t. \tag{49}$$

Similar results for $\boldsymbol{\nu}_t$ can be obtained using the same proof techniques.

□

Proposition 4 (Linearized Dynamics Approximation)**.** *For sufficiently small learning rate η, the closed-form solution admits the first-order approximation:*

$$\boldsymbol{\nu}_t \approx \left(I + t\begin{bmatrix} 0 & \gamma_B \\ \gamma_A & 0 \end{bmatrix}\right)\boldsymbol{\nu}_0, \quad \textit{where } \boldsymbol{\nu}_t \triangleq \begin{bmatrix} \nu[A^{(t)}] \\ \nu[B^{(t)}] \end{bmatrix} = \begin{bmatrix} \sigma_A^2 + t\gamma_B\sigma_B^2 \\ \sigma_B^2 + t\gamma_A\sigma_A^2 \end{bmatrix}. \tag{50}$$

This yields the update variance expansion under small-η regime:

$$\nu[W_{LoRA}^{(t)}] \approx k_1\gamma t + k_2\gamma^2 t^2, \tag{51}$$

with $\gamma = \eta^2\sigma_L^2$, $k_1 = r(m\nu[A^{(0)}]^2 + n\nu[B^{(0)}]^2)$, and $k_2 = rmn\nu[A^{(0)}]\nu[B^{(0)}]$.

Proof. For a sufficiently small learning rate η, the product $\gamma_A\gamma_B = mn\eta^4\sigma_L^4$ is very small. Hence, the eigenvalues

$$\lambda_\pm = 1 \pm \sqrt{\gamma_A\gamma_B} \tag{52}$$

can be approximated via a first-order Taylor expansion. Thus, for small t, the closed-form solution for $\boldsymbol{\nu}_t$ can be approximated as

$$\boldsymbol{\nu}_t \approx \left(I + t\begin{bmatrix} 0 & \gamma_B \\ \gamma_A & 0 \end{bmatrix}\right)\boldsymbol{\nu}_0. \tag{53}$$

By definition, we set

$$\boldsymbol{\nu}_t \triangleq \begin{bmatrix} \nu[A^{(t)}] \\ \nu[B^{(t)}] \end{bmatrix} = \begin{bmatrix} \sigma_A^2 + t\,\gamma_B\sigma_B^2 \\ \sigma_B^2 + t\,\gamma_A\sigma_A^2 \end{bmatrix}, \tag{54}$$

which agrees with the first-order expansion of the linear system. $\square$

D Analyzing LoRA-GA from Magnitude Principle

Proposition 5 (LoRA-GA initialization maximizes low-rank gradient magnitude)**.** *Given a gradient matrix $\nabla_W L \in \mathbb{R}^{n\times m}$ with SVD decomposition $\nabla_W L = USV^\top$, the optimal rank-r matrices $A \in \mathbb{R}^{r\times m}$ and $B \in \mathbb{R}^{n\times r}$ that maximize the Frobenius norm of the gradients $\|\nabla_A L\|_F^2$ and $\|\nabla_B L\|_F^2$ in Eq.* (2)*, under the constraints $\|A\|_F^2 = r$ and $\|B\|_F^2 = r$, are given by:*

$$A^\star = V_{:,:r}^\top, \quad B^\star = U_{:,:r}, \tag{55}$$

where $V_{:,:r}$ and $U_{:,:r}$ contain the first r right and left singular vectors of $\nabla_W L$, respectively.

Proof. Let $G = \nabla_W L \in \mathbb{R}^{n\times m}$ and write its SVD $G = USV^\top$ with singular values $\sigma_1 \geq \sigma_2 \geq \cdots \geq 0$. From the LoRA gradient expressions we have

$$\nabla_A L = B^\top G, \qquad \nabla_B L = GA^\top.$$

Note that $\nabla_A L$ does not depend on A and $\nabla_B L$ does not depend on B, hence the two maximization problems decouple.

(i) Maximizing $\|\nabla_B L\|_F^2$ w.r.t. A under $\|A\|_F^2 = r$. Let $A' := AV$. Then $\|A'\|_F^2 = \|A\|_F^2 = r$ and

$$\|GA^\top\|_F^2 = \|US(A')^\top\|_F^2 = \|S(A')^\top\|_F^2 = \mathrm{tr}\big(A'S^2(A')^\top\big).$$

Form the Lagrangian $\mathcal{L}(A',\lambda) = \mathrm{tr}(A'S^2(A')^\top) - \lambda(\mathrm{tr}(A'(A')^\top) - r)$. Taking derivative w.r.t. A' yields the stationarity condition $A'S^2 = \lambda A'$. Thus the rows of A' lie in the eigenspaces of S^2. To maximize the trace, one places the Frobenius norm onto the coordinates corresponding to the largest diagonal entries of S^2, i.e. the first r singular values. Taking $A'^\star = [I_r \mid 0]$ attains the maximum

$$\max_{\|A\|_F^2 = r} \|GA^\top\|_F^2 = \sum_{i=1}^{r} \sigma_i^2,$$

and $A^\star = A'^\star V^\top = V_{:,:r}^\top$ (up to orthonormal transformations within the chosen r-subspace).

(ii) Maximizing $\|\nabla_A L\|_F^2$ w.r.t. B under $\|B\|_F^2 = r$. Analogously let $B' := U^\top B$. Then

$$\|B^\top G\|_F^2 = \mathrm{tr}\big((B')^\top S^2 B'\big),$$

and the same Lagrange argument gives that the optimal choice concentrates norm on the first r coordinates, producing

$$\max_{\|B\|_F^2=r} \|B^\top G\|_F^2 = \sum_{i=1}^{r} \sigma_i^2,$$

and one may take $B^\star = U_{:,:r}$.

Hence the stated solutions $A^\star = V_{:,:r}^\top$ and $B^\star = U_{:,:r}$ are optimal, with the above maximal values. This completes the proof. □

E Details on Key Formulas

E.1 Weight Update Magnitude

$$\nu[\Delta W_{\text{LoRA}}^{(t)}] \approx r\alpha^2\eta^2 \left(\nu[B^{(t)}]\nu[\nabla_A L^{(t)}] + \nu[\nabla_B L^{(t)}]\nu[A^{(t)}]\right).$$

Proof. Given the LoRA parameter update rule:

$$\Delta W_{\text{LoRA}}^{(t)} = \alpha\eta \left(B^{(t)}\nabla_A L^{(t)} + \nabla_B L^{(t)} A^{(t)}\right) + \mathcal{O}(\eta^2), \tag{56}$$

where we retain first-order terms in η under small learning rate assumption.

Assumptions:

(A1) Independence: $B \perp\!\!\!\perp \nabla_A L$, $\nabla_B L \perp\!\!\!\perp A$

(A2) Zero-mean initialization: $\mathbb{E}[B_{ij}] = \mathbb{E}[A_{kl}] = 0$

(A3) Spatial homogeneity: $var[B_{ij}] = \nu[B]$, $var[(\nabla_A L)_{ij}] = \nu[\nabla_A L]$.

For entry (m, n) in $\Delta W_{\text{LoRA}}^{(t)}$:

$$\begin{aligned} var\left[(\Delta W)_{mn}\right] &\approx \alpha^2\eta^2 var\left[\sum_{k=1}^{r} (B_{mk}(\nabla_A L)_{kn} + (\nabla_B L)_{mk} A_{kn})\right] && (57)\\ &= \alpha^2\eta^2 \left(var\left[\sum_k B_{mk}(\nabla_A L)_{kn}\right] + var\left[\sum_k (\nabla_B L)_{mk} A_{kn}\right]\right). && (58)\end{aligned}$$

By assumptions (A1)-(A3):

$$\begin{aligned} var\left[\sum_k B_{mk}(\nabla_A L)_{kn}\right] &= \sum_k var[B_{mk}]var[(\nabla_A L)_{kn}] && (59)\\ &= r\nu[B]\nu[\nabla_A L]. && (60)\end{aligned}$$

Similarly:

$$var\left[\sum_k (\nabla_B L)_{mk} A_{kn}\right] = r\nu[\nabla_B L]\nu[A]. \tag{61}$$

Combining these terms:

$$\begin{aligned} \nu[\Delta W_{\text{LoRA}}^{(t)}] &\approx \alpha^2\eta^2 \left(r\nu[B]\nu[\nabla_A L] + r\nu[\nabla_B L]\nu[A]\right) && (62)\\ &= r\alpha^2\eta^2 \left(\nu[B]\nu[\nabla_A L] + \nu[\nabla_B L]\nu[A]\right). && (63)\end{aligned}$$

where $\nu[B]$, $\nu[A]$ inherit their magnitudes from initialization scheme, and $\nu[\nabla L]$ terms reflect task-specific loss landscape characteristics. □

E.2 Spectral Concentration Factor

Let the singular values of the pretrained weight matrix W be $\{s_i\}_{i=1}^{\mathcal{R}[W]}$. Define the average of the top-r singular values as

$$\mathbb{E}_r[s] = \frac{1}{r}\sum_{i=1}^{r} s_i, \tag{64}$$

and the average of the squares of all singular values as

$$\mathbb{E}_{\mathcal{R}[W]}[s^2] = \frac{1}{\mathcal{R}[W]}\sum_{i=1}^{\mathcal{R}[W]} s_i^2. \tag{65}$$

Because the square function is convex, Jensen's inequality implies

$$\mathbb{E}_r[s]^2 \le \mathbb{E}_r[s^2], \tag{66}$$

with equality if and only if all s_i (for $i = 1, \dots, r$) are equal. Moreover, since lower singular values generally contribute less to the overall energy, as r increases the value of $\mathbb{E}_r[s]$ decreases relative to $\mathbb{E}_{\mathcal{R}[W]}[s^2]$, making $\rho[r]$ a monotonically decreasing function of r.

E.3 Variance of A_{SVD} and B_{SVD}

Recall that the PiSSA initialization is given by

$$A_{\mathrm{SVD}} = \sqrt{S_r}\, V_{:,:r}^{\top}, \quad B_{\mathrm{SVD}} = U_{:,:r}\sqrt{S_r}, \tag{67}$$

where S_r is a diagonal matrix containing the top-r singular values of W. Assuming that the columns of V (and similarly, U) form an orthonormal basis, the variance of $V_{:,:r}$ (taken elementwise) is approximately $\nu[V_{:r}] \approx \frac{1}{m}$ (or $\frac{1}{n}$ for U), since for an orthogonal matrix the energy is uniformly distributed. Thus, the variance of A_{SVD} can be expressed as:

$$\nu(A_{\mathrm{SVD}}) = \frac{\mathrm{Tr}(\sqrt{S_r^T} V_{:,:r}^T V_{:,:r}\sqrt{S})}{mr} = \frac{\sum_{i=1}^{r} s_i}{mr} = \mathbb{E}_r[s]\nu[V_{:r}]. \tag{68}$$

To connect this with the variance of W, note that

$$\nu[W] = \frac{1}{mn}\sum_{i=1}^{\mathcal{R}[W]} s_i^2. \tag{69}$$

Thus, we can relate $\mathbb{E}_r[s]$ to $\nu[W]$ via the spectral concentration factor $\rho[r]$. Incorporating a factor of n to account for the dimensions of A_{SVD}, we obtain:

$$\nu(A_{\mathrm{SVD}}) = \sqrt{\frac{n\,\rho[r]\,\nu[W]}{m\,\mathcal{R}[W]}}. \tag{70}$$

A similar argument, with the roles of m and n interchanged, leads to the expression for $\nu(B_{\mathrm{SVD}})$.

E.4 Spectral Gain Factor

The dynamics of the LoRA weight update variance are captured by an expression of the form:

$$\nu[W_{\mathrm{LoRA}}^{(t)}] \approx k_1\gamma t + k_2\gamma^2 t^2, \tag{71}$$

where k_1 is the linear evolution rate. Substituting the variance expressions derived for A_{SVD} and B_{SVD} into the dynamical system (see Eq. (6)), we obtain:

$$k_1 = \frac{\rho[r]\, r\,(m+n)}{\mathcal{R}[W]}\,\nu[W]. \tag{72}$$

Defining

$$Q[r] \triangleq \frac{\rho[r]\, r}{\mathcal{R}[W]}, \tag{73}$$

this expression becomes:

$$k_1 = Q[r](m+n)\nu[W], \tag{74}$$

with the constraint $0 \le Q[r] \le 1$. When $\nu[W] \sim \mathcal{O}(\min(1/m, 1/n))$, the factor $Q[r]$ effectively quantifies the amplification of the weight update magnitude due to the spectral initialization.

Proof. Recall that

$$\rho[r] \triangleq \frac{\left(\frac{1}{r}\sum_{i=1}^{r} s_i\right)^2}{\frac{1}{\mathcal{R}[W]}\sum_{i=1}^{\mathcal{R}[W]} s_i^2}, \tag{75}$$

and the spectral gain factor is defined as

$$Q[r] \triangleq \frac{\rho[r]\, r}{\mathcal{R}[W]}. \tag{76}$$

Let $m = \mathcal{R}[W]$. By Jensen's inequality (or by the Cauchy–Schwarz inequality), we have

$$\left(\frac{1}{r}\sum_{i=1}^{r} s_i\right)^2 \leq \frac{1}{r}\sum_{i=1}^{r} s_i^2. \tag{77}$$

Therefore,

$$\rho[r] \leq \frac{\frac{1}{r}\sum_{i=1}^{r} s_i^2}{\frac{1}{m}\sum_{i=1}^{m} s_i^2} = \frac{m}{r}\cdot\frac{\sum_{i=1}^{r} s_i^2}{\sum_{i=1}^{m} s_i^2} \leq \frac{m}{r}, \tag{78}$$

since $\frac{\sum_{i=1}^{r} s_i^2}{\sum_{i=1}^{m} s_i^2} \leq 1$. Substituting this bound into the definition of $Q[r]$ yields

$$Q[r] = \frac{\rho[r]\, r}{m} \leq \frac{m}{r}\cdot\frac{r}{m} = 1. \tag{79}$$

This completes the proof that $Q[r] \leq 1$. □

F Further Clarifications

In this section, we provide additional details regarding the experimental setup for our theoretical validations and justify the core assumptions underlying our propositions.

F.1 Clarification on Figure 2: Experimental Setup and Optimizer Dynamics

The experiments illustrated in Figure 2 were conducted in a controlled environment to isolate and validate our theoretical claims regarding hyperparameter equivalence and magnitude dynamics. The setup uses a 5-layer MLP with an intermediate dimension of 400, where LoRA modules are trained to fit a mapping for randomly generated synthetic data. This simple setting effectively tests the fundamental fitting capabilities of LoRA.

Figure 2(a) is specifically designed to empirically validate Proposition 1, reproduced with clearer separation in Figure 6. We deliberately use two different optimizers, SGD for the first 2,500 steps and Adam thereafter, to demonstrate that when the hyperparameter product $\alpha'\alpha_A\alpha_B$ is held constant, LoRA exhibits equivalent training trajectories regardless of the optimizer. This equivalence is confirmed by the overlapping loss curves. Furthermore, the norm difference $||\Delta\tilde{W}_{\text{LoRA}}^{(t)} - \Delta W_{\text{LoRA}}^{(t)}||_F^2$ between the baseline and other equivalent settings remains near zero, confirming that the learned weights themselves evolve identically.

F.2 Clarification on Figure 3: Direct Relationship to PiSSA

The goal of Figure 3 is to visualize the source of magnitude gain in spectral initialization methods, for which we use PiSSA [40] as a representative example. The link is direct:

• The solid colored curves for the spectral concentration factor ($\rho[r]$) and spectral gain factor ($Q[r]$) are calculated directly from the SVD of the pretrained weights. This is precisely the mechanism that PiSSA employs for initialization. Therefore, these curves illustrate the inherent magnitude dynamics of a PiSSA-initialized model.

• The plots reveal two key insights from our analysis of PiSSA. First, the plot of $\rho[r]$ shows that spectral energy is highly concentrated in the top singular values, explaining why PiSSA is particularly effective at low ranks. Second, the plot of $Q[r]$ quantifies the significant magnitude gain that PiSSA (colored lines) achieves over the naive "Noise & Zeros" baseline (white dotted line). This is precisely the gain that LoRAM is designed to mimic efficiently without performing SVD.

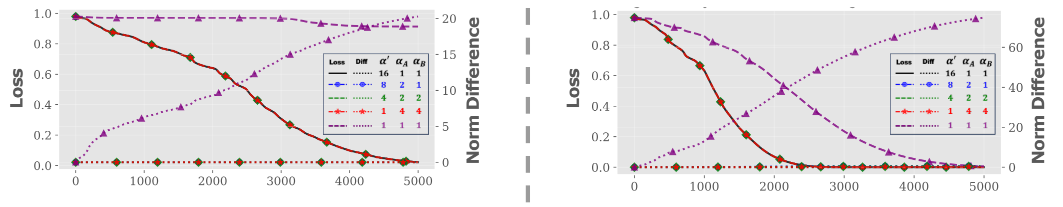

(a) SGD dynamics under different hyperparameters (b) Adam dynamics under different hyperparameters

Figure 6: A detailed view of the validation of Proposition 1, separating the SGD and Adam optimization phases. Each curve represents a model with a unique hyperparameter combination. The norm difference (right axis) aggregates the Frobenius norm discrepancies between the baseline model (black curve) and others across all layers. The results show that diverse hyperparameter sets can produce identical optimization trajectories, confirming our theoretical equivalence framework.

G Further Analysis on the Interplay of Initialization, Learning Rate, and Performance

Our primary experiments were conducted under a unified hyperparameter configuration to ensure a fair and controlled comparison. However, different initialization strategies may achieve optimal performance under varying hyperparameters, particularly the learning rate. To provide a more nuanced understanding, we conducted a supplementary analysis investigating the performance of LoRAM, PiSSA [40], and MiLoRA [41] under different learning rates.

Specifically, we compare the results from our original experiments using a moderate learning rate (2×10^{-5}) with new results obtained using a higher learning rate (2×10^{-4}), which aligns with the setting used in the original MiLoRA paper. The detailed results for ranks $r = 16$ and $r = 128$ are presented in Table 5 and Table 6, respectively.

Table 5: Performance of PiSSA, LoRAM, and MiLoRA with different learning rates at rank $r = 16$.

Learning rate	2×10^{-5}			2×10^{-4}		
Method	PiSSA	LoRAM	MiLoRA	PiSSA	LoRAM	MiLoRA
GSM8K	37.68	40.32	29.70	52.46	53.29	46.62
MATH	5.16	5.30	4.18	8.80	8.92	6.18
HumanEval	18.37	18.92	14.69	24.47	25.62	17.14
MBPP	28.62	28.83	27.23	31.22	31.74	28.65
Commonsense	73.72	75.19	67.90	77.02	79.11	76.67

Table 6: Performance of PiSSA, LoRAM, and MiLoRA with different learning rates at rank $r = 128$.

Learning rate	2×10^{-5}			2×10^{-4}		
Method	PiSSA	LoRAM	MiLoRA	PiSSA	LoRAM	MiLoRA
GSM8K	51.48	51.12	39.81	58.37	59.28	54.66
MATH	7.04	7.25	5.18	11.46	10.76	9.20
HumanEval	21.62	22.03	20.39	26.81	29.95	28.02
MBPP	31.07	31.53	29.95	36.54	37.80	33.35
Commonsense	77.28	77.81	74.29	67.09	74.23	79.01

The results reveal several key patterns:

• **At a lower rank** ($r = 16$), all methods generally benefit from the higher learning rate, showing improved performance across tasks. This suggests that in low-rank settings, a larger learning rate can enhance convergence speed.

• **At a higher rank** ($r = 128$), a clear divergence emerges. While most methods still improve, PiSSA exhibits a notable performance degradation on the Commonsense dataset. Its training loss curve in this high-rank, high-LR configuration plateaus early, suggesting that the amplified updates overshoot the effective descent direction.

• These findings align perfectly with our **magnitude principle**. PiSSA's use of principal singular components leads to stronger initial magnitude amplification, which necessitates a smaller optimal learning rate to maintain stability. Conversely, MiLoRA, which initializes with smaller minor singular components, can benefit from a larger learning rate. This analysis reinforces our claim from Section 4.3: "Magnitude scaling should be applied conservatively at higher ranks, since larger ranks inherently amplify updates."

This supplementary analysis underscores that the optimal learning rate is intrinsically linked to the magnitude scaling introduced by the initialization method.

H Efficiency Analysis: Computational and Memory Overhead

A primary motivation for LoRAM is to achieve the performance gains of spectral initialization methods while preserving the computational efficiency and minimal memory footprint of the original LoRA framework. In this section, we provide a detailed comparison of the theoretical and practical overhead associated with LoRAM, LoRA, and PiSSA.

H.1 Theoretical Complexity

The theoretical time and space complexities for the initialization phase of each method are summarized in Table 7. LoRA's overhead is minimal, stemming from random matrix initialization. LoRAM maintains this same linear complexity, as its deterministic DST basis is generated efficiently through vector multiplication. In contrast, PiSSA's complexity is dominated by the SVD of the pretrained weight matrices, a computationally intensive operation. Furthermore, PiSSA requires storing both the original and decomposed components, effectively doubling the space requirement compared to LoRA and LoRAM.

Table 7: Theoretical initialization time and space complexities of LoRA, LoRAM, and PiSSA.

Method	LoRA	LoRAM	PiSSA
Time	$O(mr + nr)$	$O(mr + nr)$	$O(\min(m^2n, mn^2))$
Space	$O(r(m + n))$	$O(r(m + n))$	$O(2r(m + n))$

H.2 Practical Performance

We empirically validated these complexities by measuring the practical initialization time and memory usage while fine-tuning LLaMA-7B on an 8-GPU server. The results, shown in Table 8, highlight two distinct workflows for PiSSA:

1. **Pre-processing :** This approach first computes and saves the residual model after subtracting the low-rank approximation. While the initialization itself is faster, this process incurs a substantial one-time storage cost, requiring over 12.5 GB to store the residual weights in addition to the LoRA adapter weights.
2. **Direct Workflow:** This method computes SVD on-the-fly, which avoids the large storage overhead. However, it is significantly slower (often taking over 10 minutes in our setup) due to known bottlenecks related to CPU-based SVD computations before GPU transfer .

As shown in the table, LoRAM's practical performance is nearly identical to that of the standard LoRA implementation, demonstrating its exceptional efficiency . It successfully eliminates the significant time and space overhead introduced by SVD-based methods like PiSSA, confirming its utility as a lightweight yet powerful initialization strategy.

I Scope and Limitations of the Magnitude Principle

While our work establishes the magnitude of weight updates as a fundamental driver of LoRA's performance, it is crucial to clearly define the scope and limitations of this principle. Our central

Table 8: Practical initialization time and space cost of LoRA, LoRAM, and PiSSA on LLaMA-7B.

Metric	**LoRA**	**LoRAM**	**PiSSA (pre-process)**	**PiSSA (direct)**
Time ($r = 16$)	1.36s	0.95s	51.32s	$>$ 10min
Time ($r = 128$)	4.23s	2.19s	57.79s	$>$ 10min
Time ($r = 512$)	8.50s	5.19s	110.31s	$>$ 10min
Space ($r = 16$)	152MB	152MB	12.5GB + 152MB	305MB
Space ($r = 128$)	1.2GB	1.2GB	12.5GB + 1.2GB	2.4GB
Space ($r = 512$)	4.8GB	4.8GB	12.5GB + 4.8GB	9.6GB

claim is that magnitude plays a **primary, not universal**, role in the success of various hyperparameter-tuning strategies. The principle provides a coherent and predictive lens for unifying these strategies, rather than suggesting that magnitude is the sole determinant of all outcomes.

The applicability and effects of magnitude scaling are subject to several important considerations:

• **Interplay with Other Hyperparameters:** As indicated by our analysis in Proposition 2, the magnitude principle is not limited to initialization magnitudes (σ_A^2, σ_B^2) alone. It is intrinsically linked to other key factors, including the LoRA rank (r), the learning rate (η), and the task-dependent gradient variance (σ_L^2). The final performance is a result of the complex interplay among all these components.

• **Interaction with Rank Size:** A key finding, highlighted in our ablation studies and consistent with our theoretical analysis, is that the benefits of magnitude scaling are not monotonic. We empirically observe that the performance gains from increased magnitude scaling tend to diminish and can even reverse at higher ranks. This is because larger ranks inherently amplify updates, as predicted by Proposition 2, suggesting that magnitude should be scaled more conservatively in high-rank settings.

• **On Optimality:** Our work aims to identify and validate update magnitude as a core mechanism influencing LoRA's training dynamics, thereby demystifying the success of methods like PiSSA. We do not claim to have identified an optimal magnitude scaling strategy. Determining the optimal magnitude for different models, tasks, and layers remains a challenging and important direction for future research.

In summary, the magnitude principle serves as a powerful analytical tool for understanding and designing LoRA-based methods, but its application should be contextualized within the broader optimization landscape.

NeurIPS Paper Checklist

1. **Claims**

   Question: Do the main claims made in the abstract and introduction accurately reflect the paper's contributions and scope?

   Answer: [Yes]

   Justification: The main claims in the abstract and introduction have clearly reflected the theoretical and empirical contributions of the paper.

   Guidelines:

   - The answer NA means that the abstract and introduction do not include the claims made in the paper.
   - The abstract and/or introduction should clearly state the claims made, including the contributions made in the paper and important assumptions and limitations. A No or NA answer to this question will not be perceived well by the reviewers.
   - The claims made should match theoretical and experimental results, and reflect how much the results can be expected to generalize to other settings.
   - It is fine to include aspirational goals as motivation as long as it is clear that these goals are not attained by the paper.

2. **Limitations**

   Question: Does the paper discuss the limitations of the work performed by the authors?

   Answer: [Yes]

   Justification: We have declared the limitations in the article, including some theoretical assumptions, and have cited relevant literature to show that these assumptions are commonly used in the field. We have also included additional technical limitations at the end of the main paper.

   Guidelines:

   - The answer NA means that the paper has no limitation while the answer No means that the paper has limitations, but those are not discussed in the paper.
   - The authors are encouraged to create a separate "Limitations" section in their paper.
   - The paper should point out any strong assumptions and how robust the results are to violations of these assumptions (e.g., independence assumptions, noiseless settings, model well-specification, asymptotic approximations only holding locally). The authors should reflect on how these assumptions might be violated in practice and what the implications would be.
   - The authors should reflect on the scope of the claims made, e.g., if the approach was only tested on a few datasets or with a few runs. In general, empirical results often depend on implicit assumptions, which should be articulated.
   - The authors should reflect on the factors that influence the performance of the approach. For example, a facial recognition algorithm may perform poorly when image resolution is low or images are taken in low lighting. Or a speech-to-text system might not be used reliably to provide closed captions for online lectures because it fails to handle technical jargon.
   - The authors should discuss the computational efficiency of the proposed algorithms and how they scale with dataset size.
   - If applicable, the authors should discuss possible limitations of their approach to address problems of privacy and fairness.
   - While the authors might fear that complete honesty about limitations might be used by reviewers as grounds for rejection, a worse outcome might be that reviewers discover limitations that aren't acknowledged in the paper. The authors should use their best judgment and recognize that individual actions in favor of transparency play an important role in developing norms that preserve the integrity of the community. Reviewers will be specifically instructed to not penalize honesty concerning limitations.

3. **Theory assumptions and proofs**

   Question: For each theoretical result, does the paper provide the full set of assumptions and a complete (and correct) proof?

Answer: [Yes]

Justification: We have provided full proofs for each proposition in the Appendix, and for the important formulas in the paper, we also give the corresponding derivation in the Appendix.

Guidelines:

- The answer NA means that the paper does not include theoretical results.
- All the theorems, formulas, and proofs in the paper should be numbered and cross-referenced.
- All assumptions should be clearly stated or referenced in the statement of any theorems.
- The proofs can either appear in the main paper or the supplemental material, but if they appear in the supplemental material, the authors are encouraged to provide a short proof sketch to provide intuition.
- Inversely, any informal proof provided in the core of the paper should be complemented by formal proofs provided in appendix or supplemental material.
- Theorems and Lemmas that the proof relies upon should be properly referenced.

4. **Experimental result reproducibility**

   Question: Does the paper fully disclose all the information needed to reproduce the main experimental results of the paper to the extent that it affects the main claims and/or conclusions of the paper (regardless of whether the code and data are provided or not)?

   Answer: [Yes]

   Justification: All benchmarks, as well as the experimental setup, are from or based on work that has been open-sourced. We have given relevant references in the paper and have given specific hyperparameter settings. Moreover, our proposed LoRAM does not require tuning parameters, as illustrated in Algorithm 1.

   Guidelines:

   - The answer NA means that the paper does not include experiments.
   - If the paper includes experiments, a No answer to this question will not be perceived well by the reviewers: Making the paper reproducible is important, regardless of whether the code and data are provided or not.
   - If the contribution is a dataset and/or model, the authors should describe the steps taken to make their results reproducible or verifiable.
   - Depending on the contribution, reproducibility can be accomplished in various ways. For example, if the contribution is a novel architecture, describing the architecture fully might suffice, or if the contribution is a specific model and empirical evaluation, it may be necessary to either make it possible for others to replicate the model with the same dataset, or provide access to the model. In general. releasing code and data is often one good way to accomplish this, but reproducibility can also be provided via detailed instructions for how to replicate the results, access to a hosted model (e.g., in the case of a large language model), releasing of a model checkpoint, or other means that are appropriate to the research performed.
   - While NeurIPS does not require releasing code, the conference does require all submissions to provide some reasonable avenue for reproducibility, which may depend on the nature of the contribution. For example
     (a) If the contribution is primarily a new algorithm, the paper should make it clear how to reproduce that algorithm.
     (b) If the contribution is primarily a new model architecture, the paper should describe the architecture clearly and fully.
     (c) If the contribution is a new model (e.g., a large language model), then there should either be a way to access this model for reproducing the results or a way to reproduce the model (e.g., with an open-source dataset or instructions for how to construct the dataset).
     (d) We recognize that reproducibility may be tricky in some cases, in which case authors are welcome to describe the particular way they provide for reproducibility. In the case of closed-source models, it may be that access to the model is limited in some way (e.g., to registered users), but it should be possible for other researchers to have some path to reproducing or verifying the results.

5. **Open access to data and code**

   Question: Does the paper provide open access to the data and code, with sufficient instructions to faithfully reproduce the main experimental results, as described in supplemental material?

   Answer: [No]

   Justification: Since we have conducted extensive experiments on several datasets, providing detailed scripts is intricate. The code will be made available upon acceptance of the article.

   Guidelines:

   - The answer NA means that paper does not include experiments requiring code.
   - Please see the NeurIPS code and data submission guidelines (`https://nips.cc/public/guides/CodeSubmissionPolicy`) for more details.
   - While we encourage the release of code and data, we understand that this might not be possible, so "No" is an acceptable answer. Papers cannot be rejected simply for not including code, unless this is central to the contribution (e.g., for a new open-source benchmark).
   - The instructions should contain the exact command and environment needed to run to reproduce the results. See the NeurIPS code and data submission guidelines (`https://nips.cc/public/guides/CodeSubmissionPolicy`) for more details.
   - The authors should provide instructions on data access and preparation, including how to access the raw data, preprocessed data, intermediate data, and generated data, etc.
   - The authors should provide scripts to reproduce all experimental results for the new proposed method and baselines. If only a subset of experiments are reproducible, they should state which ones are omitted from the script and why.
   - At submission time, to preserve anonymity, the authors should release anonymized versions (if applicable).
   - Providing as much information as possible in supplemental material (appended to the paper) is recommended, but including URLs to data and code is permitted.

6. **Experimental setting/details**

   Question: Does the paper specify all the training and test details (e.g., data splits, hyperparameters, how they were chosen, type of optimizer, etc.) necessary to understand the results?

   Answer: [Yes]

   Justification: All benchmarks, as well as the experimental setup, are from or based on work that has been open-sourced.

   Guidelines:

   - The answer NA means that the paper does not include experiments.
   - The experimental setting should be presented in the core of the paper to a level of detail that is necessary to appreciate the results and make sense of them.
   - The full details can be provided either with the code, in appendix, or as supplemental material.

7. **Experiment statistical significance**

   Question: Does the paper report error bars suitably and correctly defined or other appropriate information about the statistical significance of the experiments?

   Answer: [Yes]

   Justification: We have provided the variance of the test results, and also the range of fluctuations in the training curves.

   Guidelines:

   - The answer NA means that the paper does not include experiments.
   - The authors should answer "Yes" if the results are accompanied by error bars, confidence intervals, or statistical significance tests, at least for the experiments that support the main claims of the paper.
   - The factors of variability that the error bars are capturing should be clearly stated (for example, train/test split, initialization, random drawing of some parameter, or overall run with given experimental conditions).

- The method for calculating the error bars should be explained (closed form formula, call to a library function, bootstrap, etc.)
- The assumptions made should be given (e.g., Normally distributed errors).
- It should be clear whether the error bar is the standard deviation or the standard error of the mean.
- It is OK to report 1-sigma error bars, but one should state it. The authors should preferably report a 2-sigma error bar than state that they have a 96% CI, if the hypothesis of Normality of errors is not verified.
- For asymmetric distributions, the authors should be careful not to show in tables or figures symmetric error bars that would yield results that are out of range (e.g. negative error rates).
- If error bars are reported in tables or plots, The authors should explain in the text how they were calculated and reference the corresponding figures or tables in the text.

8. **Experiments compute resources**

   Question: For each experiment, does the paper provide sufficient information on the computer resources (type of compute workers, memory, time of execution) needed to reproduce the experiments?

   Answer: [Yes]

   Justification: Our experiments are based on a server with 8 H800 GPUs. The timing of experiments is diverse depending on the datasets, while there will be no differences between LoRAM and other approaches on the same dataset, since they do not modify the training process.

   Guidelines:

   - The answer NA means that the paper does not include experiments.
   - The paper should indicate the type of compute workers CPU or GPU, internal cluster, or cloud provider, including relevant memory and storage.
   - The paper should provide the amount of compute required for each of the individual experimental runs as well as estimate the total compute.
   - The paper should disclose whether the full research project required more compute than the experiments reported in the paper (e.g., preliminary or failed experiments that didn't make it into the paper).

9. **Code of ethics**

   Question: Does the research conducted in the paper conform, in every respect, with the NeurIPS Code of Ethics `https://neurips.cc/public/EthicsGuidelines`?

   Answer: [Yes]

   Justification: We have carefully checked and followed the NeurIPS Code of Ethics.

   Guidelines:

   - The answer NA means that the authors have not reviewed the NeurIPS Code of Ethics.
   - If the authors answer No, they should explain the special circumstances that require a deviation from the Code of Ethics.
   - The authors should make sure to preserve anonymity (e.g., if there is a special consideration due to laws or regulations in their jurisdiction).

10. **Broader impacts**

    Question: Does the paper discuss both potential positive societal impacts and negative societal impacts of the work performed?

    Answer: [NA]

    Justification: Our paper presents a general fine-tuning technique that is not specific to actual application scenarios.

    Guidelines:

    - The answer NA means that there is no societal impact of the work performed.
    - If the authors answer NA or No, they should explain why their work has no societal impact or why the paper does not address societal impact.

- Examples of negative societal impacts include potential malicious or unintended uses (e.g., disinformation, generating fake profiles, surveillance), fairness considerations (e.g., deployment of technologies that could make decisions that unfairly impact specific groups), privacy considerations, and security considerations.
- The conference expects that many papers will be foundational research and not tied to particular applications, let alone deployments. However, if there is a direct path to any negative applications, the authors should point it out. For example, it is legitimate to point out that an improvement in the quality of generative models could be used to generate deepfakes for disinformation. On the other hand, it is not needed to point out that a generic algorithm for optimizing neural networks could enable people to train models that generate Deepfakes faster.
- The authors should consider possible harms that could arise when the technology is being used as intended and functioning correctly, harms that could arise when the technology is being used as intended but gives incorrect results, and harms following from (intentional or unintentional) misuse of the technology.
- If there are negative societal impacts, the authors could also discuss possible mitigation strategies (e.g., gated release of models, providing defenses in addition to attacks, mechanisms for monitoring misuse, mechanisms to monitor how a system learns from feedback over time, improving the efficiency and accessibility of ML).

11. **Safeguards**

    Question: Does the paper describe safeguards that have been put in place for responsible release of data or models that have a high risk for misuse (e.g., pretrained language models, image generators, or scraped datasets)?

    Answer: [NA]

    Justification: The paper poses no such risks.

    Guidelines:

    - The answer NA means that the paper poses no such risks.
    - Released models that have a high risk for misuse or dual-use should be released with necessary safeguards to allow for controlled use of the model, for example by requiring that users adhere to usage guidelines or restrictions to access the model or implementing safety filters.
    - Datasets that have been scraped from the Internet could pose safety risks. The authors should describe how they avoided releasing unsafe images.
    - We recognize that providing effective safeguards is challenging, and many papers do not require this, but we encourage authors to take this into account and make a best faith effort.

12. **Licenses for existing assets**

    Question: Are the creators or original owners of assets (e.g., code, data, models), used in the paper, properly credited and are the license and terms of use explicitly mentioned and properly respected?

    Answer: [Yes]

    Justification: We have properly cited the original paper that produced the code package or dataset.

    Guidelines:

    - The answer NA means that the paper does not use existing assets.
    - The authors should cite the original paper that produced the code package or dataset.
    - The authors should state which version of the asset is used and, if possible, include a URL.
    - The name of the license (e.g., CC-BY 4.0) should be included for each asset.
    - For scraped data from a particular source (e.g., website), the copyright and terms of service of that source should be provided.
    - If assets are released, the license, copyright information, and terms of use in the package should be provided. For popular datasets, `paperswithcode.com/datasets` has curated licenses for some datasets. Their licensing guide can help determine the license of a dataset.

- For existing datasets that are re-packaged, both the original license and the license of the derived asset (if it has changed) should be provided.
- If this information is not available online, the authors are encouraged to reach out to the asset's creators.

13. **New assets**

    Question: Are new assets introduced in the paper well documented and is the documentation provided alongside the assets?

    Answer: [NA]

    Justification: The paper does not release new assets.

    Guidelines:

    - The answer NA means that the paper does not release new assets.
    - Researchers should communicate the details of the dataset/code/model as part of their submissions via structured templates. This includes details about training, license, limitations, etc.
    - The paper should discuss whether and how consent was obtained from people whose asset is used.
    - At submission time, remember to anonymize your assets (if applicable). You can either create an anonymized URL or include an anonymized zip file.

14. **Crowdsourcing and research with human subjects**

    Question: For crowdsourcing experiments and research with human subjects, does the paper include the full text of instructions given to participants and screenshots, if applicable, as well as details about compensation (if any)?

    Answer: [NA]

    Justification: The paper does not involve crowdsourcing nor research with human subjects.

    Guidelines:

    - The answer NA means that the paper does not involve crowdsourcing nor research with human subjects.
    - Including this information in the supplemental material is fine, but if the main contribution of the paper involves human subjects, then as much detail as possible should be included in the main paper.
    - According to the NeurIPS Code of Ethics, workers involved in data collection, curation, or other labor should be paid at least the minimum wage in the country of the data collector.

15. **Institutional review board (IRB) approvals or equivalent for research with human subjects**

    Question: Does the paper describe potential risks incurred by study participants, whether such risks were disclosed to the subjects, and whether Institutional Review Board (IRB) approvals (or an equivalent approval/review based on the requirements of your country or institution) were obtained?

    Answer: [NA]

    Justification: The paper does not involve crowdsourcing nor research with human subjects.

    Guidelines:

    - The answer NA means that the paper does not involve crowdsourcing nor research with human subjects.
    - Depending on the country in which research is conducted, IRB approval (or equivalent) may be required for any human subjects research. If you obtained IRB approval, you should clearly state this in the paper.
    - We recognize that the procedures for this may vary significantly between institutions and locations, and we expect authors to adhere to the NeurIPS Code of Ethics and the guidelines for their institution.
    - For initial submissions, do not include any information that would break anonymity (if applicable), such as the institution conducting the review.

16. **Declaration of LLM usage**

Question: Does the paper describe the usage of LLMs if it is an important, original, or non-standard component of the core methods in this research? Note that if the LLM is used only for writing, editing, or formatting purposes and does not impact the core methodology, scientific rigorousness, or originality of the research, declaration is not required.

Answer: [NA]

Justification: The core method development in this research does not involve LLMs as any important, original, or non-standard components.

Guidelines:

- The answer NA means that the core method development in this research does not involve LLMs as any important, original, or non-standard components.
- Please refer to our LLM policy (`https://neurips.cc/Conferences/2025/LLM`) for what should or should not be described.